








RESEARCH ARTICLE

In vitro and *in vivo* anti-epileptic efficacy of eslicarbazepine acetate in a mouse model of *KCNQ2*-related self-limited epilepsy

Laura Monni^{1,2}  | Larissa Kraus^{1,3} | Matthias Dipper-Wawra^{1,4}  |
 Patricio Soares-da-Silva^{5,6,7}  | Nikolaus Maier⁸  | Dietmar Schmitz⁸  |
 Martin Holtkamp^{1,4}  | Pawel Fidzinski^{1,2} 

¹Clinical and Experimental Epileptology, Department of Neurology, Charité-Universitätsmedizin Berlin, corporate member of Freie Universität Berlin and Humboldt-Universität zu Berlin, Berlin, Germany

²NeuroCure Clinical Research Centre, Berlin Institute of Health at Charité-Universitätsmedizin Berlin, Berlin, Germany

³Life Sciences Institute, Department of Cellular and Physiological Sciences, University of British Columbia, Vancouver, British Columbia, Canada

⁴Epilepsy-Center Berlin-Brandenburg, Institute for Diagnostics of Epilepsy, Berlin, Germany

⁵Division of Research and Development, BIAL – Portela & CA S. A, da Siderurgia Nacional, São Mamede do Coronado, Portugal

⁶Department of Biomedicine, Unit of Pharmacology and Therapeutics, Faculty of Medicine, University Porto, Porto, Portugal

⁷MedInUP, Centre for Drug Discovery and Innovative Medicines, University Porto, Porto, Portugal

⁸Neuroscience Research Centre, Charité-Universitätsmedizin Berlin, corporate member of Freie Universität Berlin and Humboldt-Universität zu Berlin, Berlin, Germany

Correspondence

Pawel Fidzinski, Clinical and Experimental Epileptology, Department of Neurology, Charité-Universitätsmedizin Berlin, corporate member of Freie Universität Berlin and Humboldt-Universität zu Berlin, Charitéplatz 1, 10117 Berlin, Germany.
 Email: pawel.fidzinski@charite.de

Present address

Larissa Kraus, Life Sciences Institute, Department of Cellular and Physiological Sciences, University of British Columbia, Vancouver, British Columbia, Canada

Funding information

Fundação Bial; NeuroCure Exzellenzcluster; NeuroCure Cluster of Excellence, Berlin Institute of Health; BIAL Portela & Ca; Eisai

Background and Purpose: The *KCNQ2* gene encodes for the $K_{v}7.2$ subunit of non-inactivating potassium channels. *KCNQ2*-related diseases range from autosomal dominant neonatal self-limited epilepsy, often caused by *KCNQ2* haploinsufficiency, to severe encephalopathies caused by *KCNQ2* missense variants. *In vivo* and *in vitro* effects of the sodium channel blocker eslicarbazepine acetate (ESL) and eslicarbazepine metabolite (S-Lic) in a mouse model of self-limited neonatal epilepsy as a first attempt to assess the utility of ESL in the *KCNQ2* disease spectrum was investigated.

Experimental Approach: Effects of S-Lic on *in vitro* physiological and pathological hippocampal neuronal activity in slices from mice carrying a heterozygous deletion of *Kcnq2* (*Kcnq2*^{+/-}) and *Kcnq2*^{+/+} mice were investigated. ESL *in vivo* efficacy was investigated in the 6-Hz psychomotor seizure model in both *Kcnq2*^{+/-} and *Kcnq2*^{+/+} mice.

Key Results: S-Lic increased the amplitude and decreased the incidence of physiological sharp wave-ripples in a concentration-dependent manner and slightly decreased

Abbreviations: 4-AP, 4-aminopyridine; aCSF, artificial cerebrospinal fluid; BFNE, self-limited familial neonatal epilepsy; CA1–3, cornu ammonis hippocampal regions 1 and 3; ESL, eslicarbazepine acetate; fEPSP, field excitatory postsynaptic potential; KCNQ, potassium channel, voltage-gated, KQT-like subfamily; S-Lic, eslicarbazepine active metabolite; SPW-R, sharp wave-ripple.

This is an open access article under the terms of the Creative Commons Attribution-NonCommercial-NoDerivs License, which permits use and distribution in any medium, provided the original work is properly cited, the use is non-commercial and no modifications or adaptations are made.

© 2021 The Authors. *British Journal of Pharmacology* published by John Wiley & Sons Ltd on behalf of British Pharmacological Society.

gamma oscillations frequency. 4-Aminopyridine-evoked seizure-like events were blocked at high S-Lic concentrations and substantially reduced in incidence at lower concentrations. These results were not different in *Kcnq2*^{+/+} and *Kcnq2*^{+/-} mice, although the EC₅₀ estimation implicated higher efficacy in *Kcnq2*^{+/-} animals. *In vivo*, *Kcnq2*^{+/-} mice had a lower seizure threshold than *Kcnq2*^{+/+} mice. In both genotypes, ESL dose-dependently displayed protection against seizures.

Conclusions and Implications: S-Lic slightly modulates hippocampal oscillations and blocks epileptic activity *in vitro* and *in vivo*. Our results suggest that the increased excitability in *Kcnq2*^{+/-} mice is effectively targeted by S-Lic high concentrations, presumably by blocking diverse sodium channel subtypes.

KEYWORDS

acute seizures models, encephalopathy, eslicarbazepine acetate, hippocampal oscillations, mouse, seizure-like event

1 | INTRODUCTION

Epilepsy is one of the most frequent neurological disorders affecting up to 1% of the population, with a lifetime prevalence of 7.6 per 1000 individuals (Fiest et al., 2017; Hirtz et al., 2007; Ngugi et al., 2010). The incidence (>60 per 100,000 individuals) of epilepsy is highest in children and at age >60 years (Fiest et al., 2017; Symonds et al., 2019). One of the major causes of childhood-onset epilepsy, and of the often associated developmental and intellectual comorbidities is the presence of mutations in the genes that control excitability and disrupt normal brain development, for example, *SCN1A* (Dravet syndrome) or *KCNQ2* (López-Rivera et al., 2020; Wheless et al., 2020). In this study, we have focused on *KCNQ2*-related diseases. The *KCNQ2* gene encodes for the **K_v7.2** subunit of **voltage-gated potassium channels**, which are expressed in various neuronal subtypes and are localized in different cell compartments (Devaux et al., 2004; Fidzinski et al., 2015; Jentsch, 2000). Homo- or heterotetrameric assemblies of K_v7.2, **K_v7.3**, and **K_v7.5** subunits form the functional channel that mediates the non-inactivating, so-called M-current (Brown & Passmore, 2009; Wang et al., 1998). The M-current is activated upon membrane depolarization and dampens neuronal excitability (Brown & Adams, 1980; Delmas & Brown, 2005; Jentsch, 2000). The clinical spectrum of *KCNQ2*-related diseases ranges from self-limited familial neonatal epilepsy (BFNE) to severe *KCNQ2* epileptic encephalopathy. BFNE is characterized by seizures occurring between days 4 and 7 of life, usually resolving within 4–6 months, with normal neurological and cognitive development (International League Against Epilepsy, ILAE; *EpilepsyDiagnosis.org*), while *KCNQ2* encephalopathy is characterized by pharmaco-resistant epilepsy and mild to profound cognitive, intellectual, and developmental impairment (Kato et al., 2013). This broad range of clinical manifestations seems to reflect different degrees of functional impairment caused by distinct variants of the *KCNQ2* gene (Goto et al., 2019; Miceli et al., 2013; Weckhuysen et al., 2012; reviewed by Nappi

What is already known

- In paediatric patients, *KCNQ2*-related diseases range from self-limited epilepsy to severe encephalopathy with pharmaco-resistant seizures.
- Eslicarbazepine acetate has good tolerability and anti-epileptic efficacy in adult forms of epilepsy.

What this study adds

- Eslicarbazepine alters hippocampal oscillations and seizure-like events in a *Kcnq2*^{+/-} mouse model of self-limited epilepsy.
- *In vivo*, eslicarbazepine acetate showed anti-epileptic efficacy also in the increased hyperexcitability *Kcnq2*^{+/-} mice phenotype.

What is the clinical significance

- Eslicarbazepine effects on hippocampal oscillations may clarify the mechanisms underlying the side effects on cognition.
- Eslicarbazepine acetate efficacy in *Kcnq2*^{+/-} mice represents the beginning of alternative treatments for childhood epilepsies.

et al., 2020). According to literature, BFNE is mostly caused by stop-gain mutations with the primary pathogenic mechanism relying on haploinsufficiency (Goto et al., 2019; Miceli et al., 2013). In contrast, *KCNQ2* epileptic encephalopathy is mostly caused by *de novo* *KCNQ2* missense variants (Goto et al., 2019; Kato et al., 2013) resulting in a dominant-negative M-current suppression (Jentsch, 2000; Miceli et al., 2013).

At onset, patients suffering from the mild BFNE phenotype are effectively treated with anti-epileptic drugs (AEDs) such as [phenobarbital](#) or [carbamazepine](#), and in the further course of the disease, seizure remission occurs regardless of treatment (Grinton et al., 2015; Sands et al., 2016). On the other hand, most patients with *KCNQ2* encephalopathy continue to suffer from pharmaco-resistant epilepsy and accompanying neurodevelopmental impairments (Goto et al., 2019; Miceli et al., 2013; Weckhuysen et al., 2012; reviewed by Nappi et al., 2020). The anti-epileptic potential of sodium channel blockers such as carbamazepine and [phenytoin](#) is well known (Beckonert et al., 2018; Doeser et al., 2015; Pisano et al., 2015; Sands et al., 2016). Within the sodium channel blocker family of anti-epileptic drugs, [eslicarbazepine acetate \(ESL\)](#) is a rather novel anti-epileptic drug, which, together with carbamazepine and [oxcarbazepine](#), belongs to the dibenzazepine family (Benes et al., 1999; Soares-da-Silva et al., 2015). The principal mechanism of ESL is to block the [voltage-gated sodium channels](#) by prolonging their slow inactivation state (Hebeisen et al., 2015; Soares-da-Silva et al., 2015). ESL is currently approved as adjunctive and monotherapy in adults with focal-onset seizures by the European Medicines Agency (EMA), the Food and Drug Administration (FDA) and Health Canada (Trinka et al., 2018). Recently, a phase-II trial has shown positive effects of ESL as adjunctive treatment in children and adolescents aged 6–16 years, reducing seizure frequency without negative effects on neurocognitive and behavioural functions (Jóźwiak et al., 2018).

Given good tolerability and the positive therapeutic potential of ESL, we aimed to investigate ESL efficacy in the *KCNQ2* disease spectrum. Here, we choose to use a well-characterized and available loss-of-function mouse model of *KCNQ2*-related self-limited epilepsy, as a first step towards assessment of ESL efficacy in *KCNQ2* loss-of-function related diseases including severe *KCNQ2* encephalopathies.

The chosen model carries a deletion in the *Kcnq2* gene that leads to a lack of expression of the *KCNQ2* protein (Watanabe et al., 2000). Homozygous (*Kcnq2*^{-/-}) mice die shortly after birth due to pulmonary atelectasis, while their heterozygous littermates (*Kcnq2*^{+/-}) show a normal lifespan, no significant behavioural abnormalities and no spontaneous epileptic seizures. However, the reduced expression of the *KCNQ2* protein in *Kcnq2*^{+/-} mice results in an increased vulnerability to epileptogenic stimuli, either chemically or electrically induced, such as the pentylenetetrazol (PTZ) or 6-Hz corneal stimulation model, respectively (Otto et al., 2009; Watanabe et al., 2000). We hypothesize that inhibition of sodium channels by ESL might be effective in reducing an increased excitability underlying seizures in *KCNQ2*-related epilepsy. Specifically, we employed the *Kcnq2*^{+/-} mouse model to investigate *in vitro* effects of S-Lic, eslicarbazepine active metabolite, on physiological hippocampal network oscillations such as sharp wave-ripple complexes (SPW-Rs), gamma oscillations and pathological seizure-like events. In addition, we exploited the 6-Hz psychomotor seizure *in vivo* model to test the anti-seizure efficacy of ESL in *Kcnq2*^{+/-} and *Kcnq2*^{+/+} mice.

2 | METHODS

2.1 | Animals

All experimental procedures were conducted in accordance with the European Directive 2010/63/EU and the German Animal Welfare Act for animal experiments and were approved by the Institutional Animal Welfare Officer and the responsible local authorities (Landesamt für Gesundheit und Soziales Berlin, licence numbers: T0265/17, G0078/18). Particular attention was paid in order to reduce the number of animals used and their suffering. Heterozygous (*Kcnq2*^{+/-}) mice with C57BL/6J background (RRID:IMSR_HAR:2000) and carrying a deletion in *Kcnq2* gene from position 418 to 535 were crossed with wild-type (*Kcnq2*^{+/+}) mice to avoid the birth of *Kcnq2*^{-/-} animals that die around perinatal age (Watanabe et al., 2000). Wild-type littermates were used as control for all *in vitro* and *in vivo* experiments. Mice were maintained under controlled environmental enriched conditions, with 12-h light/dark cycle (6:00 h/18:00 h), on wooden litter with *ad libitum* access to food and water. Up to nine animals of the same sex were kept in the same individually ventilated cage. Animal studies are reported in compliance with the ARRIVE v2.0 guidelines (Percie du Sert et al., 2020) and with the recommendations made by the *British Journal of Pharmacology* (Lilley et al., 2020).

2.2 | Hippocampal slice preparation

All *in vitro* experiments were performed in hippocampal slices from juvenile (P28–32) *Kcnq2*^{+/+} and *Kcnq2*^{+/-} mice (20–25 g). Slice preparation was conducted as previously described (Heuzeroth et al., 2019) with minimal modifications. Briefly, mice were anaesthetised with isoflurane and decapitated, and the brain was quickly removed and kept in ice cold (1–4°C) artificial cerebrospinal fluid (aCSF), continuously carbogenated (95% O₂, 5% CO₂). aCSF contained in mM: NaCl 125.0, KCl 2.0, MgCl₂ 1.0, CaCl₂ 2.0, NaH₂PO₄ 1.25, NaHCO₃ 25.0, and glucose 10.0 (pH 7.4, 300 ± 10 mOsm). The cerebellum was then removed and the hemispheres separated and glued to a vibratome chamber. 400-µm-thick horizontal brain slices were cut from both hemispheres with a vibratome (Leica VT1200S, Wetzlar, Germany) and contained the entorhinal cortex (EC), the subiculum (SUB), the dentate gyrus (DG), and the cornu ammonis regions 1, 2, and 3 (CA1, CA2, and CA3). Before starting of the electrophysiological recording, slices were allowed to recover for at least 1 h in an Haas-type interface chamber (Haas et al., 1979), continuously perfused with prewarmed (35°C) and carbogenated aCSF at 1.6 ml·min⁻¹.

2.3 | Local field potential recordings

Spontaneous sharp wave-ripples (SPW-Rs), kainate-induced gamma oscillations and seizure-like events evoked by 4-AP were all recorded via extracellular local field potential recordings. Borosilicate pipettes

(Science Products, Hofheim, Germany; 1.5 mm outer diameter) were pulled with a vertical puller (PC-10, Narishige, Tokyo, Japan; electrode resistance 1–2 M Ω) and filled with 154-mM NaCl.

SPW-R activity was recorded from CA1 pyramidal layer of ventral hippocampal slices perfused with prewarmed ($\sim 35 \pm 0.5^\circ\text{C}$) and carbogenated aCSF (Kubota et al., 2003; Maier et al., 2003, 2009; Papatheodoropoulos & Kostopoulos, 2002). The recordings were performed in a modified submerged-type recording chamber with high flow rate (10 ml·min $^{-1}$) (Hill & Greenfield, 2011; Kraus et al., 2020). The signal was sampled at 20 kHz, low-pass filtered at 2 kHz, and digitized by a Digidata1550 interface and processed by PClamp10 software (Molecular Devices, Sunnyvale, CA, USA, RRID:SCR_011323). Baseline activity was recorded for ≥ 30 min (SPW-R incidence ~ 1 Hz). Eslicarbazepine metabolite (S-Lic) was added at a concentration of 0 (0.12% DMSO as vehicle control), 10, 30, 100, and 300 μM , respectively, randomly assigned to one slice per mouse each. During drug application, SPW-R activity was recorded for ≥ 30 min; thereafter, the drug was washed out, and the activity recorded for further ≥ 30 min.

Gamma oscillations were induced by adding kainate (100 nM) (Schneider et al., 2015; Wójtowicz et al., 2009). These recordings were performed from CA3 and CA1 pyramidal layers in an interface chamber in which slices were placed on a transparent membrane (culture plate inserts 0.4 μm Millicell; Millipore, Bedford, MA, United States). Signals were sampled at 10 kHz and acquired by custom-made amplifiers (10 \times) connected to an AD converter (Micro 1401 mk II, Cambridge Electronic Design Limited, Cambridge, UK). Data were processed with Spike2 and Signal (versions 7.00 and 3.07, respectively; Cambridge Electronic Design Limited, Cambridge, UK, RRID:SCR_000903 and SCR_014276, respectively). Baseline was recorded for ≥ 60 min, and S-Lic was then added to aCSF at a concentration of 0 (0.12% DMSO as vehicle control) and 300 μM , randomly assigned to one slice per mouse each. S-Lic was applied and the activity was recorded for ≥ 30 min. Finally, the drug was washed out and activity recorded for further ≥ 40 min.

Input/output (I/O) curves and field excitatory postsynaptic potentials (fEPSP)/population spike coupling were measured in submerged conditions in the presence of 300- μM S-Lic to evaluate effects of S-Lic on synaptic transmission and intrinsic excitability, respectively. A bipolar stimulating electrode (1–2 M Ω) placed in the stratum (st.) radiatum was used to evoke fEPSPs recorded from st. radiatum at more distal CA1 location. Stimulus intensity was increased and adjusted progressively and three independent measurements were done for each stimulus in order to get the desired amplitude of the fibre volley (Fidzinski et al., 2015). In all I/O curve experiments, we examined fEPSPs slope (20–80% of the maximum) in order to minimize contamination by the PS. For fEPSP/PS coupling, two recording electrodes placed in the pyramidal cell layer and the dendritic layer of CA1 were used. Stimulation intensity was adjusted to achieve the maximal fEPSP slope (approx. 1.6–2 mV·ms $^{-1}$). fEPSP slopes were determined 1 ms prior to the population spike, while population spike amplitude was defined as the absolute difference between population spike peak and anti-peak.

Seizure-like events were recorded in submerged conditions as previously reported, with some modifications (Heuzeroth et al., 2019). Epileptiform activity was induced by application of 4-AP (100 μM), a non-selective potassium channel blocker (Avoli et al., 1993; Perreault & Avoli, 1992), and field potentials were recorded from the entorhinal cortex (Lopantsev & Avoli, 1998). Typically, an *in vitro* seizure-like event evoked with 4-AP appears as a negative field potential shift characterized by the presence of low-amplitude gamma-activity. This activity is then followed by sustained tonic events and terminates with rhythmic bursting that slows down in frequency while increasing in amplitude (Avoli et al., 1993). Here, seizure-like events were identified with the following electrographic features: (1) duration of the negative field potential shift ≥ 10 s; (2) field potential decrease of ≥ 0.5 mV; (3) a seizure-like event starts with a single spike preceding the negative shift and ends with the termination of the rhythmic bursting. The signal was sampled at 10 kHz, low-pass filtered at 2 kHz by a Digidata 1550, and processed by PClamp10 software. Baseline activity was recorded for ≥ 30 min. Then S-Lic was added to the epileptogenic aCSF at a concentration of 0 (0.12% DMSO as vehicle control), 30, 100, and 300 μM , randomly assigned to one slice per mouse, and activity was recorded for ≥ 30 min, followed by a wash-out of ≥ 30 min.

For all *in vitro* experiments, blinding of the experimenter was not possible due to technical reasons, though statistical analysis explained in the last section of methods was conducted in a blinded fashion.

2.4 | 6-Hz psychomotor seizure model

The 6-Hz psychomotor seizure model is employed to induce *in vivo* acute seizures in rodents, which are thought to resemble pharmacoresistant seizures (Barton et al., 2001; Brown et al., 1953). *Kcnq2* $^{+/+}$ and *Kcnq2* $^{+/-}$ mice (P21–P28) were employed to test the effect of ESL on seizures evoked by 6-Hz corneal stimulation. All animals were acclimated to the experimenter 1 week before stimulation and to the experiment room for ≥ 1 h before the experiment started. A topical anaesthetic (0.4% **oxybuprocaine hydrochloride**, Omnivision GmbH, Puchheim, Germany) was applied to both eyes of the mouse to provide local anaesthesia 3 min before corneal stimulation (0.2-ms duration of rectangular pulses for 3 s at 6 Hz). The stimulation was applied via corneal electrodes connected to a constant current pulse generator (ECT Unit 5780, Ugo Basile, Comerio, Italy). The electrodes were wetted with 0.9% saline before each stimulation in order to secure a good electrical contact. Before investigating ESL effects, a total of 40 animals (four subgroups with 10 animals each: male *Kcnq2* $^{+/+}$, male *Kcnq2* $^{+/-}$, female *Kcnq2* $^{+/+}$, female *Kcnq2* $^{+/-}$) was used to determine the CC $_{50}$ and CC $_{97}$ for seizure induction by using the staircase technique previously described by Barton et al. (2001). Briefly, mice were stimulated two or three times every 48 h with increasing current intensities ranging between 8 and 24 mA. Stimulations were excluded from probit analysis when it was not possible to determine the presence of a clear seizure, either because of failure in the electrode conductance detection by

the pulse generator or no clear response from the animal. After determination of the CC₉₇ for the two genotypes, the effects of ESL was tested in 20 *Kcnc2*^{+/+} and 40 *Kcnc2*^{+/-} male mice (20 mice stimulated with 1.5-fold *Kcnc2*^{+/-}-CC₉₇ and 20 mice stimulated with 1.5-fold *Kcnc2*^{+/+}-CC₉₇). Sample size was estimated according to previous studies demonstrating a minimum of five to nine animals for sufficient statistic certainty (probability of type II errors <20%) and to reduce animal number to a minimum following 3Rs approach (Vittinghoff & McCulloch, 2007). Each animal was stimulated twice every 72 h, during which the general animal welfare and potential signs of stress were monitored every day. ESL dose (0, 10, 30, and 100 mg·kg⁻¹) was randomly administered via oral gavage (administration volume 10 ml·kg⁻¹) approximately 60 min before stimulation. Immediately after stimulation, mice were placed in an open small cage (dimensions: 25 × 20 × 14 cm) for observation. Seizure intensity was scored by using a modified Racine's scale: 0, no behavioural changes; 1, sudden arrest with orofacial automatism; 2, sudden arrest with head nodding; 3, forelimb clonus; 4, forelimb clonus with rearing and possibly falling; 5, generalized tonic-clonic activity with loss of postural tone and sporadic wild jumping (Ihara et al., 2016; Racine, 1972). Experimenters were blinded for mice genotype during the whole experiment and for mice genotypes and ESL doses during follow-up scoring process. All mice were sacrificed at the end of the experiment by decapitation under isoflurane anaesthesia. Whole brain and plasma were collected and frozen at -80°C for the analysis of S-Lic concentration.

2.5 | Rotarod test

The rotarod test was used as a preliminary screening for a possible ESL toxicity on motor coordination (Dunham & Miya, 1957). Sixty minutes after ESL oral administration, mice were placed on a rotating rod (Ugo Basile, model 47600) for a maximum of 2 min at a constant speed of 15 rpm. Two trials were done for each mouse, interrupted by a 5-min break. The trial was considered failed if the mouse was not able to maintain its balance for at least 10 s, and it was placed back on the rod for a maximum of three times. The time that a mouse was able to rotate without falling or rotating by grasping onto the drum was recorded.

2.6 | Analyses of the S-Lic metabolite in plasma, whole brain and hippocampal slices

S-Lic concentrations in plasma and tissue (whole brain and hippocampal slices) were determined using a validated enantioselective LC-MS/MS assay (6470, Triple Quad LC-MS Agilent Technologies, Santa Clara, CA, USA) as previously described (Loureiro et al., 2011). In brief, plasma samples (50 µl) were thawed at 4°C, added to 100 µl of internal standard working solution (ISTD; 2000 ng·ml⁻¹ of 10,11-dihydrocarbamazepine in phosphate buffer pH 5.6) and

processed by extraction of solid phase. Samples were agitated by using a vortex and centrifuged for 10 min at 20,000 g. Finally, the supernatant was transferred to HPLC vials/plates to be injected into the LC-MS/MS. Whole brain samples (without cerebellum) and hippocampal slices were thawed at 4°C and weighed. Water was added to obtain a tissue concentration of 0.1 g·ml⁻¹. Subsequently, samples were homogenized by using a Heidolph DIAX 900 mixer and transferred to 1.5-ml Eppendorf tubes. Samples were centrifuged for 30 min at 10,000 g at 4°C, and 50 µl of supernatant was added to 100-µl ISTD working solution and then processed by extraction of solid phase. In the same manner as for plasma, brain tissue samples were agitated with a vortex and centrifuged for 10 min at 20,000 g. Finally, the supernatant was filtered and transferred HPLC vials/plates to be injected into the LC-MS/MS. The samples were quantified with the analytical calibration range of 10.0 to 5000.0 ng·ml⁻¹, both for plasma and brain tissues. The limit of quantification was 10.0 ng·ml⁻¹.

2.7 | Data processing and statistical analyses

The data and statistical analysis comply with the recommendations and requirements on experimental design and analysis in pharmacology (Curtis et al., 2018). SPW-Rs, gamma oscillations, and seizure-like events raw data were analysed with custom-written MATLAB scripts (R2014b, R2016b, MathWorks, Natick, MA, USA, RRID:SCR_001622). For SPW-Rs and gamma oscillations, the last 10 and 5 min of each condition were examined, respectively. For seizure-like events, the last 25 min of each condition were considered for statistical analysis. The different frequency components of SPW-Rs were addressed separately. The slower sharp wave component was detected by low-pass filtering the raw local field potential recording at 50 Hz, and a threshold was set at 3.5 times the standard deviation of baseline free of events. The faster ripple component was detected by filtering the raw data at 80–600 Hz, and a threshold was fixed at 3.5 times the standard deviation of the filtered and smoothed data. Analysed parameters were incidence (events s⁻¹) and amplitude (mV) of sharp waves and ripples. Finally, for CA1 SPW-Rs, the peak amplitudes of sharp waves and ripples were carried out. The correlation coefficients were then calculated for each sharp wave and ripple amplitude pair.

Gamma frequency (Hz) and power spectral density (PSD, µV²·Hz⁻¹) were calculated by first dividing the raw data vector into 10-s bins, obtaining the spectrogram by using Chronux toolbox functions (<http://chronux.org/>, RRID:SCR_005547; Bokil et al., 2010; Mitra & Bokil, 2008). Data were then processed with Welch's based fast Fourier transform for the calculation of power spectra in the 30–48 Hz frequency band. The temporal relationship between CA3 and CA1 regions during gamma oscillation activity was analysed by investigating the gamma phase, cross-correlation, and time lag. To this end, the last 5 min of each condition (baseline, treatment, and washout) from CA3 and CA1 recordings were first notch-filtered at 50 Hz in the frequency domain. Data were then down-sampled to 5 kHz and band-pass filtered (1–100 Hz). Stretches of 5 s were

cross-correlated by using MATLAB “xcorr” function, and the resulting cross-correlation functions were normalized such that the auto-correlations at zero lag were equivalent to 1, and finally averaged. The averaged cross-correlation peaks, along with their lags, were compared across the experimental conditions.

Data obtained from *in vivo* staircase test used to assess the CC₉₇ and their 95% confidence intervals for the 6-Hz psychomotor seizure model were calculated using the probit analysis (Finney, 1971). For the *in vivo* seizure scoring process, two experimenters blindly gave a

score to each mouse response to the current stimulus, and the average of the two scores was considered for the statistical analysis. Correlation analysis was performed to investigate the relationship between seizure score and S-Lic concentration in plasma and whole brain. Simple linear regression analysis was used to investigate differences between the coefficient of determination (r^2) of *in vitro* and *in vivo* data of follow-up measurements of S-Lic concentration in brain tissue. EC₅₀ values were calculated with AAT Bioquest web software (EC50 Calculator|AAT Bioquest).

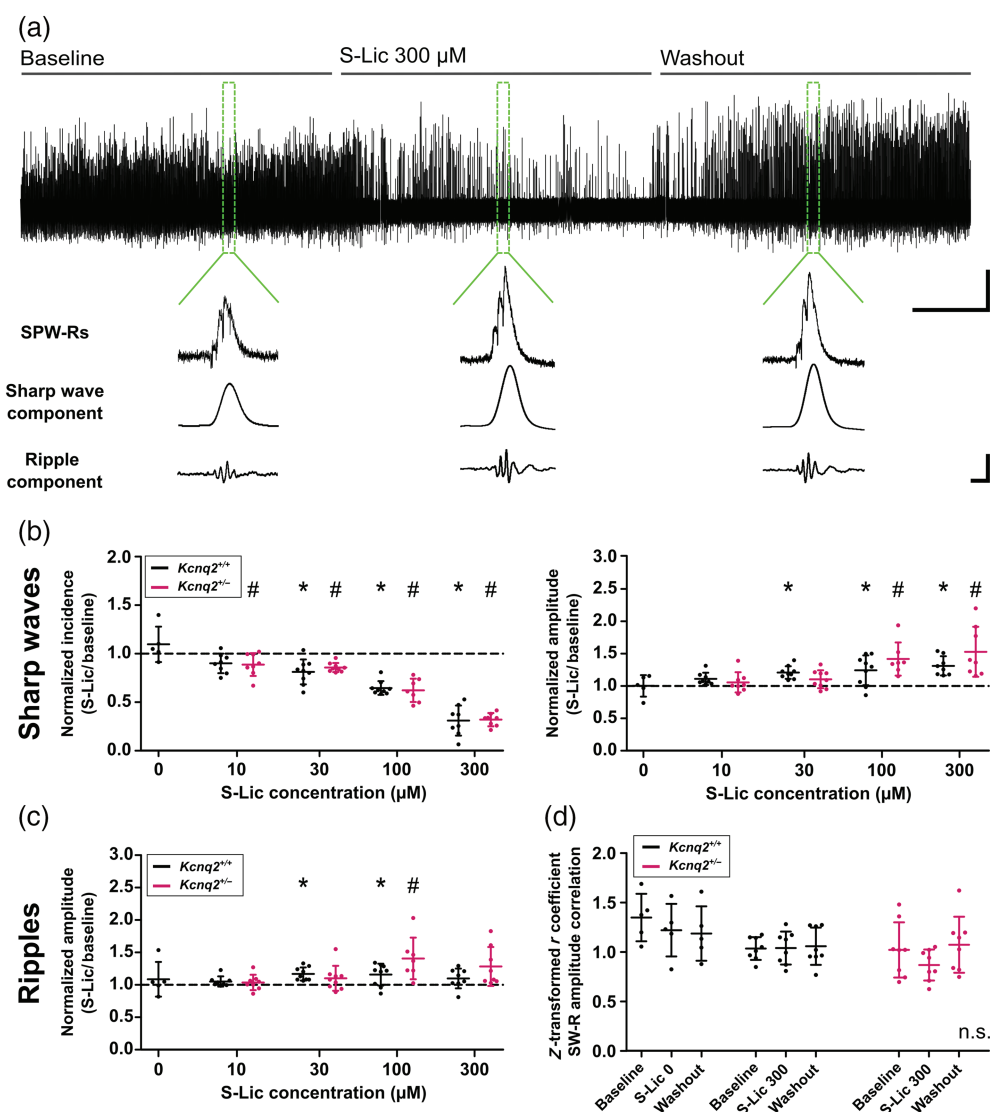


FIGURE 1 S-Lic effects on sharp wave-ripples (SPW-Rs) *in vitro* in the CA1 region. (a) Top: Representative extracellular recording from CA1 pyramidal layer. Bottom: Examples of single SPW-R events including low-pass (30 Hz; sharp wave component) and band pass (80–250 Hz; ripple component) filtered traces during baseline, S-Lic 300 μM and washout, respectively. Scale bars: 5 min, 0.2 mV; 20 ms, 0.2 mV. (b,c) Scatter plots showing incidence (left panel) and amplitude (right panel) of sharp waves component (b) and ripples component amplitude (c). In each graph, vehicle controls (S-Lic 0) and four different S-Lic concentrations are displayed. (d) Scatter plots showing the z-transformed coefficients of correlation between the amplitude of ripples and sharp waves, during baseline and upon application of vehicle control or S-Lic 300 μM, respectively, and washout. Each dot refers to one slice obtained from one animal, data are shown as mean ± standard deviation. Data in (b) and (c) are normalized to the baseline. Asterisks and number signs mark statistically significant differences between treatment and correspondent baseline as assessed by one-way ANOVA or Friedman test and Tukey's or Dunnett's post hoc test for multiple comparisons, respectively (P value ≤ 0.05). $Kcna2^{+/+}$: $n = 5, 8, 9, 9,$ and 8 , for vehicle control and four S-Lic concentrations, respectively; $Kcna2^{+/-}$: $n = 8, 9, 7,$ and 8 , for four S-Lic concentrations, respectively

Statistical analysis was conducted for experiment group sizes of $n \geq 5$ independent values, referred to biological samples. *In vitro* experiments were designed to be conducted in groups of equal size ranging 5–10 independent samples. In some cases, group size was unequal due to the necessity to evoke stable events such as SPW-Rs, gamma oscillations, or seizure-like events throughout the recording. With the exception of the analysis of the CA3-CA1 temporal relationship during gamma oscillations presented in Figure S2, all power calculations were performed a priori. Sample size was estimated in order to reach a power of 80% with an effect size of 20–25%. In case of the CA3-CA1 temporal relationship, the statistical power calculation was performed a posteriori and revealed that these experiments are underpowered and that a slightly higher number of replicates would have been required. All data were analysed with GraphPad Prism 5 (GraphPad Software Inc., San Diego, CA, USA, RRID: SCR_002798). Prior to statistical evaluation, all data were subjected to D'Agostino and Pearson omnibus normality test or Kolmogorov–Smirnov normality test (when $n < 8$) and further analysed accordingly. Correlation and cross-correlation coefficients of sharp wave and ripple amplitudes and gamma oscillations, respectively, were transformed with the Fisher z-transformation to generate a Gaussian-distributed dataset. The results were expressed as z-transformed r coefficient and z-transformed CrossCorr, respectively. For normally distributed data, statistical analysis was carried out using repeated measurements (for electrophysiological data) one-way analysis of variance (ANOVA) and post hoc Tukey's test for multiple comparisons. Two-way ANOVA and post hoc Bonferroni's test were used to compare data across genotypes. Post hoc tests were run only if ANOVA F value attained the required level of statistical significance, and there was no significant inhomogeneity in variance tested with the Bartlett's test for equal variances. The Pearson coefficient was applied for correlation analysis of normally distributed data. In case the normality test was not passed, the Friedman non-parametric test for repeated measurements or the Kruskal–Wallis test were used, with post hoc Dunnett's multiple comparison of individual groups. The Spearman coefficient was applied for correlation analysis of non-normally distributed data. Circular statistics was used to analyse gamma oscillation phase data with NCSS Statistical Software (2021, NCSS, LLC, Kaysville, Utah, USA, ncss.com/software/ncss). Data of gamma phase from both $Kcng2^{+/+}$ and $Kcng2^{+/-}$ mice showed unequal Von Mises concentration factor (κ); therefore, data were analysed with the nonparametric Uniform Score test.

A P value ≤ 0.05 was considered as statistically significant for all analyses. Normally distributed and normalized data to control for unwanted sources of variation are shown as mean \pm standard deviation (SD). Data of SPW-Rs and seizure-like events are shown as normalized to baseline (Figures 1b,c and 4b, respectively) only for illustrative purposes. Normalized data were expressed as ratio between treatment and baseline. We excluded one data point from the gamma oscillations time lag analysis due to technical reasons, namely, the presence of positive spikes that precluded the correct detection needed for calculating time lag.

2.8 | Materials

Eslicarbazepine acetate [(–)-(S)-10-acetoxy-10,11-dihydro-5H-dibenzo/b,f/azepine-5-carboxamide] and its metabolite eslicarbazepine (referred also to as [S]-licarbazepine, S-Lic) [(+)-(S)-10,11-dihydro-10-hydroxy-5H-dibenzo/b,f/azepine-5-carboxamide] were synthesized and tested by BIAL Portela & Ca, S.A., with purities $>99.5\%$. Kainic acid (kainate) was employed to evoke *in vitro* gamma oscillations and was purchased from Cayman Chemical Company, Ann Arbor, MI, USA. 4-Aminopyridine (4-AP), a non-selective potassium channel blocker, was used to induce *in vitro* seizure-like events and was obtained from Sigma, Munich, Germany. The vehicle used to dissolve eslicarbazepine acetate for *in vivo* oral administration was 0.2% hydroxypropylmethylcellulose (HPMC) dissolved in distilled water, while dimethyl sulfoxide (DMSO, max concentration 0.12%) was used to dissolve the metabolite eslicarbazepine to a stock concentration of 250 mM for *in vitro* experiments. Both HPMC and DMSO were obtained from Sigma.

2.9 | Nomenclature of targets and ligands

Key protein targets and ligands in this article are hyperlinked to corresponding entries in the IUPHAR/BPS Guide to PHARMACOLOGY <http://www.guidetopharmacology.org> and are permanently archived in the Concise Guide to PHARMACOLOGY 2020/21 (Alexander et al., 2021).

3 | RESULTS

3.1 | S-Lic reduces sharp wave incidence and increases SPW-R amplitude

Sharp wave–ripple complexes (SPW-Rs) consist of high frequency (~ 200 Hz) “ripple” oscillations superimposed on slow (~ 5 –10 Hz) waves (sharp waves). *In vivo*, SPW-Rs are observed during slow wave sleep and immobility and are thought to play an important role in a variety of cognitive functions (including memory consolidation) (Buzsáki, 1986; for review, see Buzsáki, 2015, and Maier & Kempter, 2017). Previous studies have established *in vitro* models of SPW-Rs facilitating the investigation of synaptic mechanisms underlying these events (Kubota et al., 2003; Maier et al., 2003; Papatheodoropoulos & Kostopoulos, 2002). Here, we applied SPW-Rs as a readout parameter to assess the effect of S-Lic on functional synchronization in hippocampal networks. SPW-Rs were recorded from CA1 pyramidal layer (Figure 1a). The application of S-Lic significantly and reversibly reduced SPW-R incidence in a concentration-dependent manner (Figure 1b, left panel) in both $Kcng2^{+/+}$ and $Kcng2^{+/-}$ mice. In addition, S-Lic increased SPW-R amplitude (Figure 1b, right panel, and Figure 1c). Control experiments with 0.12% DMSO left SPW-Rs unaffected. The amplitude of sharp waves and ripples recorded in CA1

pyramidal layer were strongly and positively correlated in both *Kcnq2^{+/+}* and *Kcnq2^{+/-}* mice. Moreover, the comparison between z-transformed correlation coefficients revealed analogous correlation of sharp waves and ripples amplitude, even upon application of the highest S-Lic concentration (Figure 1d).

3.2 | S-Lic alters properties of hippocampal gamma oscillations

Gamma oscillations occur in the frequency range of 30–90 Hz (Buzsáki & Wang, 2012; Freeman, 2007). They are implicated in many different cognitive functions, for example, episodic memory retrieval and exploratory behaviour (Csicsvari et al., 2003; Montgomery & Buzsáki, 2007). In our study, gamma oscillations *in vitro* in

hippocampal CA3 and CA1 area were evoked via activation of **ionotropic glutamate receptors** with kainate (Figure 2a-1) (Buhl et al., 1998). Application of 300- μ M S-Lic reduced the mean oscillation frequency in CA3 and CA1 both in *Kcnq2^{+/+}* and in *Kcnq2^{+/-}* mice (Figure 2c). We did not find any systematic change in gamma spectral power upon application of S-Lic (Figure S1).

We then analysed S-Lic effects on the synchronization and temporal relationship between CA3 and CA1 during gamma oscillations *in vitro* and found that the gamma phase was largely unaffected by S-Lic (Figure S2A), while cross-correlation between CA3 and CA1 decreased during application of S-Lic (Figure S2B). Similarly, the time lag between CA3 and CA1 significantly increased in the presence of the drug (Figure S2C). We have to note, however, that this post hoc analysis was slightly underpowered as detailed in the Methods section.

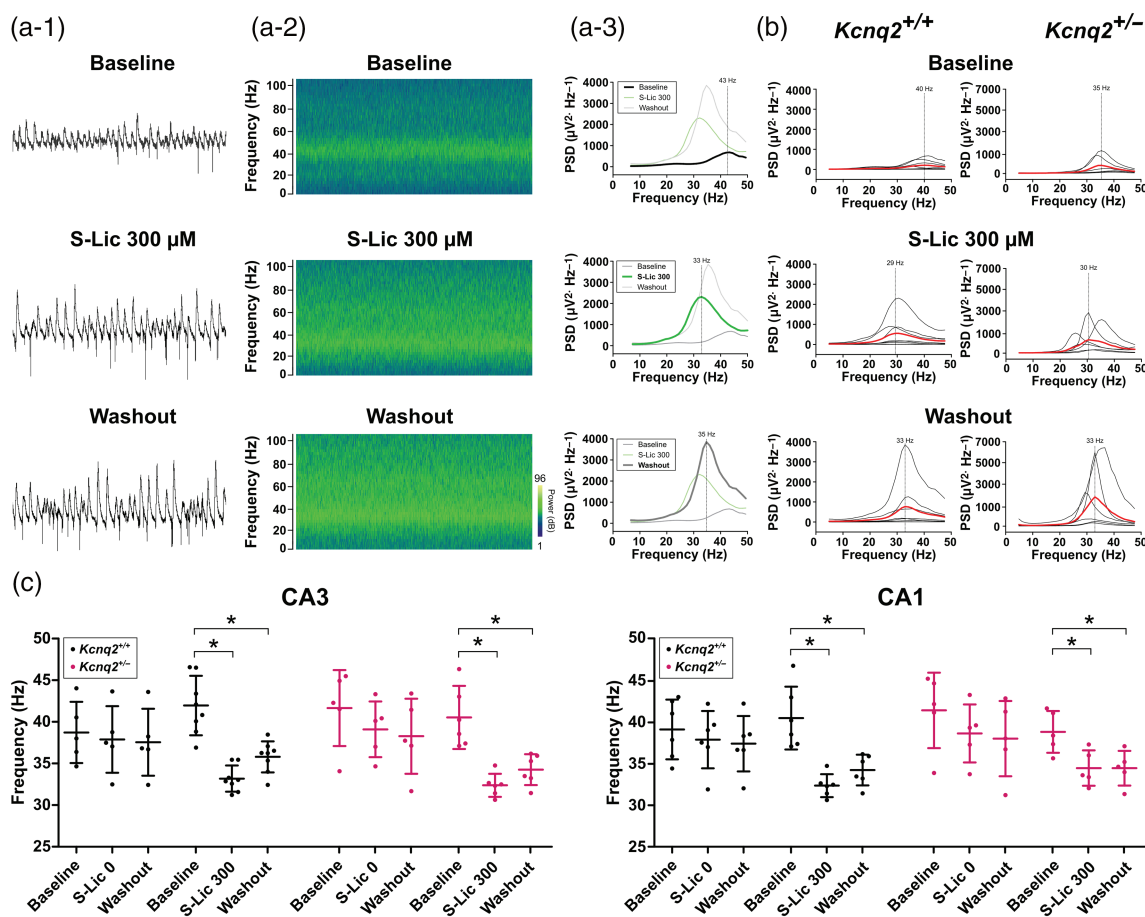


FIGURE 2 S-Lic effects on gamma oscillations *in vitro* in the CA3 region. (a-1) Representative traces of kainate-induced gamma oscillations recorded from pyramidal layer of CA3 mouse hippocampal slice. Top: baseline; middle: S-Lic 300 μ M, bottom: washout. Scale bar: 100 ms, 0.5 mV. (a-2) Wavelet spectrograms of the same example trace depicted in a-1. Scale bar: 1 min. Lighter colours represent higher power. (a-3) Power spectra for the example traces depicted in a-1. Vertical lines denote mean peak of gamma frequency. (b) Power spectra for all experiments recorded from CA3 (each line represents one experiment) obtained during baseline (top), application of S-Lic 300 μ M (middle) and washout (bottom) from *Kcnq2^{+/+}* (left) and *Kcnq2^{+/-}* (right) slices. Thicker red lines represent mean of all experiments for a given condition. Vertical lines denote mean peak of gamma frequency. (c) Scatter plots showing the frequency of gamma oscillations recorded from CA3 (left panel) and CA1 (right panel), upon application of vehicle control (S-Lic 0) and S-Lic 300 μ M. *Kcnq2^{+/+}*: S-Lic 300 n = 8, S-Lic 0 n = 5; *Kcnq2^{+/-}*: S-Lic 300 n = 6, S-Lic 0 n = 5

3.3 | S-Lic does not affect input/output behaviour and intrinsic excitability in the CA1 area

Interplay between synaptic inhibition and excitation is critical for the network synchronization during hippocampal population activity such as SPW-Rs and gamma rhythm (Atallah & Scanziani, 2009; Buzsáki, 2015; Kubota et al., 2003; Maier et al., 2003). Recording of input/output (I/O) and fEPSP/population spike coupling relationships provide insights in basal properties of synaptic transmission and excitation-to-inhibition coupling in the region of interest, respectively. Therefore, to gain insight into possible target mechanisms underlying the effect of S-Lic on neuronal oscillations, we firstly conducted extracellular I/O recordings in the CA1 area in the absence and presence of S-Lic. Post-synaptic fEPSP slopes at given fibre volley amplitudes (Figure 3a) were not different between wild-type and heterozygous *Kcnq2* mice. Likewise, application of S-Lic did not affect synaptic input behaviour in either genotype (Figure 3a-1,a-2).

We also performed fEPSP/population spike coupling experiments to assess S-Lic effects on intrinsic excitability (Figure 3b). Similar to I/O recordings, S-Lic did not alter population spike amplitude in neither genotype. Of note, also no differences were detected between genotypes (Figure 3b-1,b-2).

3.4 | S-Lic reduces *in vitro* seizure-like events frequency in a concentration-dependent manner

A well-established model to study synaptic foundations of pathological network synchronization is the 4-AP acute model of epileptiform activity (Avoli et al., 1993; Losi et al., 2016; Perreault & Avoli, 1992; Rudy, 1988). Upon exposure to 100- μ M 4-AP, local field potential recordings from entorhinal cortex exhibited stable seizure-like events in brain slices from both *Kcnq2*^{+/+} and *Kcnq2*^{+/-} mice (Figure 4a). As depicted in Figure 4b, S-Lic effectively and concentration-

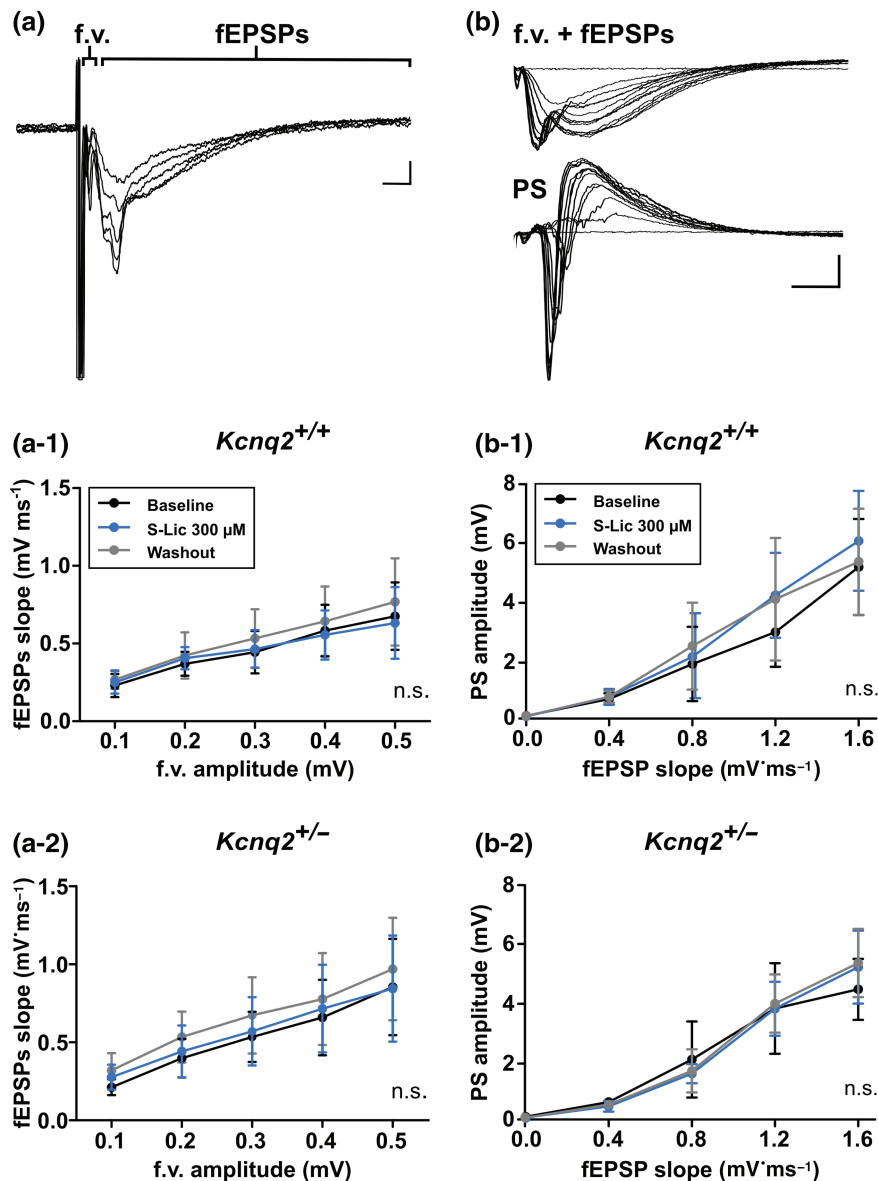


FIGURE 3 S-Lic does not affect I/O properties and intrinsic excitability in the CA1 region *in vitro*. (a) Example recording of fibre volley (f.v.) and the consequent field excitatory postsynaptic potential (fEPSP) responses recorded from the CA1 st. radiatum at five different stimulation intensities. Scale bar: 5 ms, 0.2 mV. (a-1, a-2) Line graphs showing recorded fEPSPs slopes in relation to f.v. amplitudes during baseline, S-Lic and washout in *Kcnq2*^{+/+} (a-1) and *Kcnq2*^{+/-} (a-2). Dots and lines represent mean fEPSPs slopes \pm standard deviation for a given f.v. amplitude. n.s. = not significant difference between the groups ($n = 8$) as assessed by two-way ANOVA. (b) Example recordings showing fibre volleys (f.v.) with consequent fEPSPs from the CA1 st. radiatum of hippocampal slices (top) and the corresponding population spikes (PS) recorded from CA1 pyramidal cell layer (bottom). Scale bar: 5 ms, 1 mV. (b-1, b-2) Line graphs displaying changes of PS amplitude in relation to fEPSPs slope during baseline, S-Lic and washout in *Kcnq2*^{+/+} (b-1) and *Kcnq2*^{+/-} (b-2). Dots and lines represent mean PS amplitudes \pm standard deviation for a given fEPSPs slope. n.s. = not significant difference between the groups ($n = 5$) as assessed by two-way ANOVA

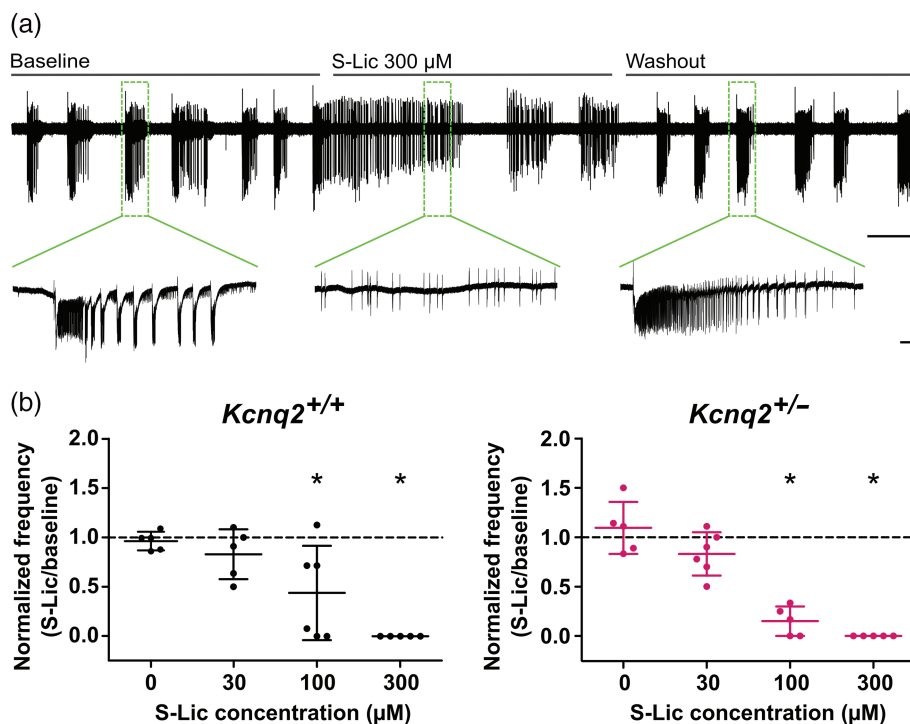


FIGURE 4 S-Lic effects on 4-AP induced seizure-like events *in vitro*. (a) Top: Representative high-pass-filtered recording showing seizure-like events (SLEs) induced by 4-AP from the entorhinal cortex. Bottom: SLE example during baseline (left), near-complete absence of SLEs during application of S-Lic (middle) and reappearance during washout (right). Scale bars: 5 min, 0.5 mV; 10 s, 0.5 mV. (b) Scatter plots showing normalized frequency of SLEs subjected to vehicle control (S-Lic 0) and three different concentrations of S-Lic for *Kcnq2*^{+/+} (left) and *Kcnq2*^{+/-} (right) slices. Each dot refers to one slice obtained from one animal; data are shown as mean \pm standard deviation. Asterisks mark statistically significant differences between treatment and correspondent baseline as assessed by one-way ANOVA or Friedman test and Tukey's or Dunnett's post hoc test for multiple comparisons, respectively (P value \leq 0.05). *Kcnq2*^{+/+}: $n = 5, 5, 6,$ and $5,$ respectively, *Kcnq2*^{+/-}: $n = 5, 6, 5,$ and $5,$ respectively

TABLE 1 S-Lic EC₅₀ and ED₅₀ values calculated from *in vitro* and *in vivo* experiments

	<i>In vitro</i>		<i>In vivo</i>	
	Experiment S-Lic EC ₅₀ (μ M)	Follow-up S-Lic EC ₅₀ (μ g·ml ⁻¹)	Experiment ESL ED ₅₀ (μ M)	Follow-up S-Lic EC ₅₀ (μ g·ml ⁻¹)
<i>Kcnq2</i> ^{+/+}	73.8	10.42 (41 μ M)	33.0	0.94 (4 μ M)
<i>Kcnq2</i> ^{+/-}	55.3	10.52 (41 μ M)	67.4	1.53 (6 μ M)

Note: EC₅₀ and ED₅₀ values calculated from experiments data are depicted in the first column (*in vitro* experiments) and third column (*in vivo* experiments). EC₅₀ values obtained from follow-up measurements of the drug metabolite concentration in brain tissue are shown in the second column (hippocampal slice tissue from *in vitro* experiments) and in the fourth column (whole brain from *in vivo* experiments).

independently blocked seizure-like event activity in both genotypes. Of note, 100- μ M S-Lic effectively reduced seizure-like event incidence in all slices from *Kcnq2*^{+/-} mice but only in 50% of slices from *Kcnq2*^{+/+} mice. Consistently, calculation S-Lic EC₅₀ revealed a lower value for *Kcnq2*^{+/-} when compared to *Kcnq2*^{+/+} mice (Table 1, first column).

3.5 | Decreased seizure threshold in *Kcnq2*^{+/-} mice in the 6-Hz psychomotor seizure model

As S-Lic was effective in suppressing seizure-like events *in vitro* and as the results suggested a slightly higher efficacy on *Kcnq2*

heterozygous mice, we extended our investigation to an *in vivo* approach. To this end, we applied the 6-Hz psychomotor seizure model, considered as a model of pharmaco-resistant seizures (Barker-Haliski et al., 2018; Barton et al., 2001). This model was previously used to demonstrate a reduced seizure threshold in *Kcnq2*^{+/-} mice compared to *Kcnq2*^{+/+} littermates when using 1.5- to 2-fold amplitude of the CC₉₇ convulsive current. Using the staircase method described by Barton et al. (2001), mice from both sexes and both genotypes were stimulated with increasing current intensities (8–24 mA). Subsequent probit analysis confirmed previous results by revealing decreased seizure threshold for male *Kcnq2*^{+/-} mice (*Kcnq2*^{+/+}: CC₅₀ = 17.1 mA, 95% CI 16.2–17.9 mA; *Kcnq2*^{+/-}:

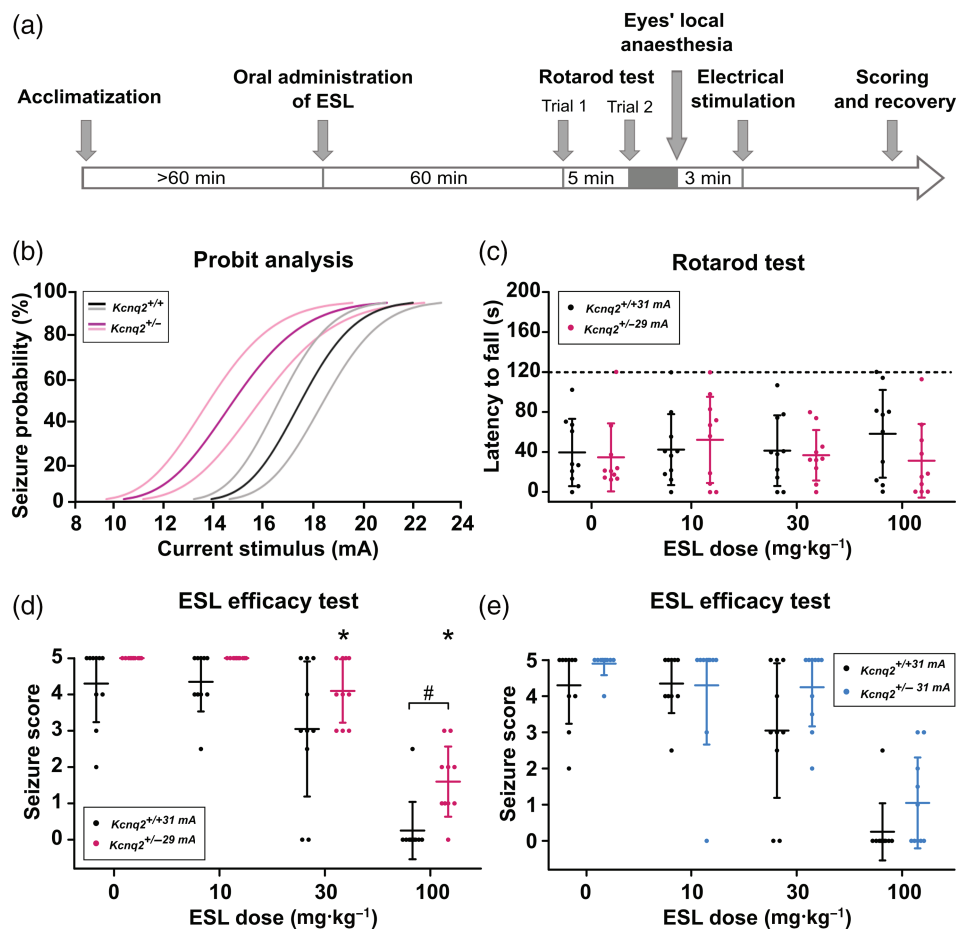


FIGURE 5 Efficacy of ESL in the 6-Hz psychomotor seizure model *in vivo*. (a) Graphical visualization of the time line employed for the 6-Hz psychomotor seizure *in vivo* experiments. Arrows indicate time points. (b) Seizure probability in dependence from stimulation intensity shown as line graphs calculated with the probit analysis. Black/grey and red/pink lines represent mean data \pm 95% confidence interval from *Kcnq2*^{+/+} and *Kcnq2*^{+/-} mice, respectively ($n = 23$; $n = 16$ respectively). (c) Rotarod test results expressed as time to fall and shown as scatter plots with data from different ESL doses including vehicle control ($n = 10$). Each dot represents the mean of two trials. (d, e) Seizure scores (0–5) at different ESL doses. (d) Seizure scores for genotype-specific CC_{97} . (e) Comparison of ESL effect on seizure score in both genotypes stimulated with $1.5 \times CC_{97}$ of *Kcnq2*^{+/+} (same *Kcnq2*^{+/+} group in d and e). Each dot refers to the mean of the scores given to one stimulated animal observed by two experimenters during follow-up blinded seizure scoring process. Data are shown as mean \pm standard deviation ($n = 10$). Asterisks mark statistically significant differences between ESL doses of each genotype assessed by one-way ANOVA and Dunnett's post hoc test for multiple comparisons. Number signs mark statistically significant differences between genotypes assessed by two-way ANOVA and Bonferroni's post hoc test (P value ≤ 0.05)

$CC_{50} = 14.5$ mA, 95% CI 13.6–15.5 mA) (Figure 5b). In female mice, probit analysis was not possible due to high variability of responses in the *Kcnq2*^{+/+} group (data not shown). Subsequent investigation of ESL effects was performed exclusively in male animals.

3.6 | ESL protects against acute seizures *in vivo* without affecting motor coordination

The anti-epileptic effects of ESL *in vivo* were tested in the 6-Hz psychomotor seizure model using 1.5-fold CC_{97} stimulation intensity, which has been proved to be adequate for the screening of anti-epileptic drug efficacy (Barker-Haliski et al., 2018; Barton et al., 2001); 1.5-fold CC_{97} was calculated from the staircase procedure separately

for each genotype: 31 mA for *Kcnq2*^{+/+} and 29 mA for *Kcnq2*^{+/-} mice. Sixty minutes after drug administration and shortly before stimulation, the Rotarod test was employed as screening for motor coordination. No difference in latency to fall was detected between mice that received ESL and mice that received the vehicle control (Figure 5c). Likewise, no difference was detected between *Kcnq2*^{+/+} and *Kcnq2*^{+/-} genotypes. ESL exerted anti-epileptic effects in a dose-dependent manner in both genotypes (Figure 5d). Upon administration of $100 \text{ mg} \cdot \text{kg}^{-1}$ ESL, 9 out of 10 tested *Kcnq2*^{+/+} mice did not display seizures (seizure score = 0) and the remaining animal showed a sudden arrest (seizure score = 2.5). In contrast, in the *Kcnq2*^{+/-} group, only 1 out of 10 animals remained seizure-free while the remaining 9 individuals displayed seizure in a score range 1–3. Of note, in the control group that received only vehicle, we observed a

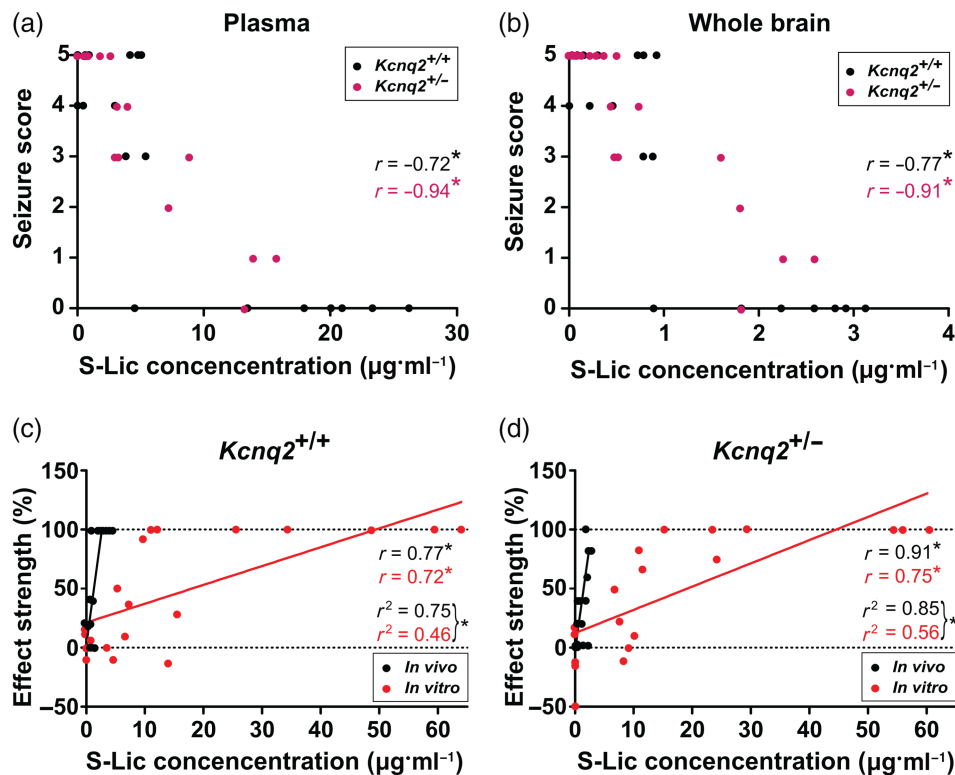


FIGURE 6 S-Lic concentration in plasma and whole brain and comparison between *in vitro* and *in vivo* correlation. (a, b) Dot plots displaying the relationship between seizure score assessed during 6 Hz psychomotor seizure model and S-Lic concentration in plasma (a) and whole brain tissue (b). Each dot refers to one plasma or whole brain sample obtained from one animal ($n = 20$). r : corresponding colour-coded correlation coefficients. Asterisks mark statistical significance assessed by correlation analysis (P value ≤ 0.05). (c, d) Correlation of anti-epileptic effect strength and S-Lic concentration *in vitro* and *in vivo*, for $Kcnq2^{+/+}$ (c) and $Kcnq2^{+/-}$ (d) mice. Dot plots display relationship between S-Lic concentration and anti-epileptic effect strength given in %. r and r^2 : corresponding colour-coded correlation coefficients and coefficients of determination for each group, respectively. Each dot refers to one hippocampal slice ($n = 20$) or whole brain ($n = 20$) sample obtained from one animal. Asterisks mark statistical significance assessed by correlation analysis (P value ≤ 0.05). Statistically significant differences between black and red best-fit lines slope assessed by linear regression analysis: $F(1, 36) = 30.6$, $P \leq 0.05$ ($Kcnq2^{+/+}$); $F(1, 36) = 22.3$, $P \leq 0.05$ ($Kcnq2^{+/-}$)

tendency of $Kcnq2^{+/-}$ mice to display a higher seizure score. Moreover, ED_{50} for $Kcnq2^{+/-}$ mice was higher than $Kcnq2^{+/+}$ mice (Table 1, third column). To exclude that these effects were due to different stimulation intensities (genotype-specific CC_{97}), we repeated the experiment in an additional group of $Kcnq2^{+/-}$ mice using the same stimulation intensity that was applied in $Kcnq2^{+/+}$ animals (31 mA). Here, we found that the seizure score difference remained unaltered (Figure 5e). Taken together, our results confirmed that $Kcnq2^{+/-}$ mice displayed a lower seizure threshold and demonstrated that ESL is effective in these animals.

3.7 | S-Lic concentration correlates with efficacy *in vivo* and *in vitro*

Correlation analysis was applied to investigate the relationship between S-Lic concentration in plasma and whole brain and the seizure scores of mice exposed to 6-Hz stimulation. In line with the expected anti-seizure efficacy of ESL, S-Lic concentration in

both plasma and brain was significantly and negatively correlated to the seizure score in either genotype (Figure 6a,b). Statistical analysis was then applied to compare S-Lic concentrations in brain tissue from *in vitro* and *in vivo* experiments with the respective effect strength (Figure 6c,d). Effect strength was determined separately for each hippocampal slice or investigated animal as the relative drug efficacy in suppressing seizure-like or seizure activity. For *in vitro* experiments, effect strength was calculated as $[(1 - \text{seizure-like event frequency drug}/\text{seizure-like event frequency baseline}) \times 100]$. For *in vivo* experiments, the seizure scores were considered equivalent to effect strength of: 5 = 0%; 4 = 20%; 3 = 40%; 2 = 60%; 1 = 80%; 0 = 100%. In either genotype, S-Lic concentration was positively correlated with its effect strength both *in vitro* and *in vivo* (Figure 6c,d). Linear regression analysis showed a statistically significant difference between the best-fit lines of *in vitro* and *in vivo* data from both genotypes (Figure 6c,d). In addition, EC_{50} values revealed that substantially higher concentrations of S-Lic are required *in vitro* (Table 1, second and fourth columns).

4 | DISCUSSION

In the present study, we investigated the effects of the anti-epileptic drug ESL and its major active metabolite S-Lic in a mouse model of KCNQ2-related childhood epilepsy (Watanabe et al., 2000). In both *Kcnq2*^{+/+} and *Kcnq2*^{+/-} slice preparations, (1) S-Lic modified SPW-Rs complexes and (2), to a lesser degree also gamma oscillations, (3) S-Lic did not affect input/output properties or fEPSP/population spike coupling in CA1, but (4) effectively reduced 4-AP induced seizure-like events. *In vivo*, (5) ESL reduced seizure incidence and score in the 6 Hz psychomotor seizure model. Also, (6) *Kcnq2*^{+/-} mice displayed a decreased seizure threshold and decreased sensitivity to ESL, while (7) no effects of ESL on motor coordination were detected. Finally, (8) S-Lic concentrations negatively correlated with seizure score *in vivo* and revealed (9) differences between effective S-Lic concentrations *in vitro* and *in vivo*.

4.1 | Eslicarbazepine effects on hippocampal oscillations

SPW-Rs and gamma oscillations play critical roles in a variety of cognitive functions. While SPW-Rs are involved in consolidation of long-term memory, gamma oscillations are considered to coordinate neuronal activity in the CA3 and CA1 regions and modulate higher cognitive functions (Csicsvari et al., 2003; Montgomery & Buzsáki, 2007).

The decreased incidence and increased amplitude of SPW-R in the CA1 region in both genotypes indicate an impact of S-Lic on rhythm generators. S-Lic did not alter synaptic or intrinsic properties in field recordings, which is in line with previous findings (Booker et al., 2015). At the single cell level, S-Lic modulates the slow inactivation of *Na_v1.2* and *Na_v1.6* sodium channels (Booker et al., 2015; Holtkamp et al., 2018). However, these effects might be too subtle to be detected at the level of field potential recordings.

S-Lic decreased gamma frequency without affecting its power and likely decreased the cross-correlation between CA3 and CA1 without affecting the gamma phase. Previous studies point to gamma generators in the entorhinal cortex and the CA3 area inducing high- and low-frequency gamma oscillations, respectively (Bragin et al., 1995; Colgin et al., 2009). Although slightly underpowered, our supplemental data on cross-correlation and time lag between CA3 and CA1 point to a downtrend impact of S-Lic on their temporal relationship, potentially due to less precise neuronal spiking. Mechanistically, S-Lic mediated inhibition of sodium channels likely affects feedback regulation between principal neurons and interneurons, critical for synchronization of gamma oscillations (Fisahn et al., 1998). The lacking wash-out effect (Figures 2c and S1) is possibly due to enhanced synaptic activity induced by gamma oscillations in excitatory synapses, leading to enlarged presence of SPW-Rs after wash-out of kainate or *carbachol* (Zarnadze et al., 2016). Persistent gamma activity might lead to a boost of gamma power itself and a decrease of the gamma frequency. In our study, the gamma power continuously increased also in long-term (2 h) control experiments.

Effects of S-Lic on neuronal oscillations are possibly associated with cognitive side effects observed with high doses of eslicarbazepine acetate. Of note, therapeutic S-Lic concentrations in plasma samples from patients are lower (by a magnitude of ~10) than what was used in our *in vitro* experiments (Hebeisen et al., 2015). Despite the fact that the M-current is implicated in hippocampal network synchronization underlying SPW-Rs, gamma and theta oscillations (Cooper et al., 2001), our *in vitro* experiments did not reveal differences between the two investigated genotypes. The *K_v7.2* subunit is highly expressed in hippocampal interneurons, which modulate excitability and synchronization during oscillations (Cooper et al., 2001). In a recent study, *K_v7.2/7.3* channel inhibition was shown to increase SPW-Rs incidence (Trompoukis et al., 2020). Also, *K_v7.5* channels have been demonstrated to control excitability through modulation of synaptic activity and loss of *Kcnq5* gene expression caused a reduction in gamma oscillations and ripples *in vivo* (Fidzinski et al., 2015). The lack of differences between genotypes in our study is possibly due to a compensatory increase in *K_v7.2* expression, a phenomenon that was observed before in adult mice heterozygous for the *Kcnq2* gene (Robbins et al., 2013). Although we employed juvenile mice (≤4 weeks), which are more susceptible to epileptogenic stimuli *in vivo* (Watanabe et al., 2000), it is possible that this “compensatory” mechanism was already taking place, which might explain the absence of clear differences between the genotypes seen throughout the application of S-Lic during SPW-Rs and gamma oscillations. This slow, age-dependent recurrence of the M-current might have also impacted pathological seizure-like events *in vitro*, though to a lower extent.

4.2 | S-Lic reduces *in vitro* seizure like-events in both genotypes

In contrast to mild S-Lic effects on physiological oscillations *in vitro*, S-Lic massively reduced the incidence of seizure-like events. Interestingly, at submaximal concentrations (100 μM), S-Lic was more effective in *Kcnq2*^{+/-} mice when compared to *Kcnq2*^{+/+} littermates. The spike threshold in *Kcnq2*^{+/-} mice is lower (Otto et al., 2009; Watanabe et al., 2000), and it might have been effectively counteracted by sodium channel inhibition by S-Lic. It is unclear whether the increased efficacy of S-Lic in slices from affected animals is specific—we did not test S-Lic in other *in vitro* models such as high potassium or low magnesium (Mody et al., 1987; Traynelis & Dingledine, 1988) due to their long-term instability. The 4-AP *in vitro* model of acute seizure-like events used in our study leads to stable activity over hours and is sensitive to a variety of anti-epileptic drugs (Heuzeroth et al., 2019). However, application of 4-AP presents a massive pro-epileptic stimulus, which might also explain differences of S-Lic EC₅₀ between *in vivo* (4–6 μM) and *in vitro* (41 μM) conditions. Finally, an important limitation of an *in vitro* acute model of seizure-like events in contrast to epileptic animals is the lack of a genuine epileptic network (Heuzeroth et al., 2019)—*in vitro* seizure-like events reflect electrographic features but not seizures.

4.3 | ESL is effective against acute seizures in the 6-Hz psychomotor seizure model

In line with previous studies (Otto et al., 2009; Watanabe et al., 2000), we confirmed a decreased seizure threshold in *Kcnq2*^{+/-} male mice. Results from female mice were variable and precluded proper staircase/probit analysis, possibly due to hormonal cycle influence on neuronal excitability and seizure threshold (Scharfman & MacLusky, 2006). In males, ESL protected mice of both genotypes against acute seizures evoked by 1.5-fold CC₉₇ in a dose-dependent manner. ESL efficacy at the highest dose (100 mg·kg⁻¹) was more robust in *Kcnq2*^{+/+} than in *Kcnq2*^{+/-} mice. This difference prevailed also when *Kcnq2*^{+/-} mice were stimulated with 1.5-fold CC₉₇ of *Kcnq2*^{+/+} animals. The results point to a genotype-dependent ESL efficacy and further confirm that seizure threshold is decreased in *Kcnq2*^{+/-} mice.

ESL doses in the present work were chosen according to previous studies (Booker et al., 2015; Hebeisen et al., 2015). Using 2xCC₉₇ (44 mA), the mentioned studies revealed an ED₅₀ in the range of 12–16 mg·kg⁻¹. Taking into account the limited number of doses employed, we estimated an ED₅₀ of 33 and 67.4 mg·kg⁻¹ for *Kcnq2*^{+/+} and *Kcnq2*^{+/-} mice, respectively, indicating a lower relative ESL efficacy in *Kcnq2*^{+/-} animals. We did not test ESL doses >100 mg·kg⁻¹. Our results confirm that ESL has a strong anti-convulsant effect in the 6-Hz psychomotor seizure model and indicates increased drug resistance in *Kcnq2*^{+/-} mice. As reported previously by others, ESL doses employed in our study did not affect motor coordination (Doeser et al., 2015; Hebeisen et al., 2015).

In the 6-Hz psychomotor seizure model, widely used to assess anti-convulsant effects of different anti-epileptic drugs (Barton et al., 2001; Hebeisen et al., 2015; Leclercq & Kaminski, 2015), the genetic background can strongly influence the seizure score and resistance to drugs (Barker-Haliski et al., 2018). The mice employed in our study had a C57Bl/6J background, while Leclercq and Kaminski, as well as Hebeisen et al., used NMRI mice. These two mouse lines have been reported to have a comparable seizure threshold but a different level of seizure resistance to phenytoin and **levetiracetam** (Leclercq & Kaminski, 2015). The higher seizure scores in *Kcnq2*^{+/-} compared to *Kcnq2*^{+/+} mice are in line with increased neuronal excitability in *Kcnq2*^{+/-} mice that apparently is easier to detect *in vivo*. Potentially, preserved connectivity in the brain *in vivo* might be required for the full manifestation of network effects derived from the reduced expression of channels containing K_v7.2 subunits (Otto et al., 2009).

4.4 | Comparison of S-Lic efficacy in *in vitro* and *in vivo* experiments

The effective S-Lic concentration in brain tissue is ~10× lower *in vivo* than in experiments conducted *in vitro* (Figure 6 and Table 1), which is in line with previous studies showing (1) a low brain/plasma ratio due to low capability of S-Lic in crossing the blood-

brain barrier (Alves et al., 2008) and (2) plasma/tissue distribution in *in vitro* experiments (Hebeisen et al., 2015). S-Lic has a half-life of 13–20 h and peaks at 1–3 h (Almeida et al., 2008). Since whole brains were sampled ~60 min after oral administration, we can exclude that the metabolite was already subjected to clearance. Therefore, even if the EC₅₀/ED₅₀ values in this study are estimations that could not be statistically analysed according to pharmacological standards (Jiang & Kopp-Schneider, 2015), they point to differences of substance efficacy between *in vitro* and *in vivo* preparations.

In previous studies, ESL was effective at comparable concentrations to those applied in our work. *In vivo*, ESL 100 mg·kg⁻¹ prevented acute seizures and epilepsy in the latrunculin A mouse model and prevented paroxysmal activity in EEG recordings, indicating a possible anti-epileptogenic effect (Sierra-Paredes et al., 2014). In a **pilocarpine** rat model, Doeser et al. postulated a protective effect of ESL (150–300 mg·kg⁻¹) against chronically induced epileptic activity and development of repetitive seizures *in vitro* and *in vivo* (Doeser et al., 2015). ESL (30–100 mg·kg⁻¹) anti-seizure efficacy was also demonstrated in corneal and amygdala kindling models of focal-onset seizures (Potschka et al., 2014). Hebeisen and colleagues investigated *in vitro* anti-seizure activity of S-Lic at 30, 100, and 300 μM in hippocampal slices from wild-type mice and revealed ESL (50, 100, and 150 mg·kg⁻¹) efficacy in the MES and 6-Hz psychomotor models *in vivo*. Further, the analysis of ESL metabolites in whole brain tissue and plasma revealed comparable concentrations between tissue S-Lic concentration and ESL doses used in *in vivo* experiments (Hebeisen et al., 2015). In our work, we have additionally provided a demonstration of the expected effective concentrations in *in vitro* experiments and the difference reported in *in vivo* conditions.

4.5 | Limitations of the *Kcnq2* mouse model

In our study, we used juvenile animals in order to apply the 6-Hz model that is not established for neonates. The chosen age presents a limitation as the use of animals shortly after birth would have better reflected the early disease onset in KCNQ2-related disorders in patients. Overall, acute epilepsy models present a limitation per se—chronic models with spontaneous recurrent seizures are more adequate. Peters and colleagues developed a mouse model with a conditional dominant negative *Kcnq2* transgene, which causes the suppression of the M-current and spontaneous seizures (2005), but these mice showed features inconsistent with the human phenotype. In other *Kcnq2* mutations such as A306T, adult seizures occur in 16% of patients, but this mutation has been characterized only for some BFNE families (Singh et al., 2008). The *Kcnq2* heterozygous mouse model developed by Watanabe and colleagues was advantageous in terms of similarities in network features underlying KCNQ2-related epilepsy (Otto et al., 2009; Watanabe et al., 2000). Therefore, by choosing to investigate *in vitro* and *in vivo* ESL effects in a model of BFNE, we sought to provide first preclinical data for a

possible choice of this compound as anti-seizure treatment also for the more severe *KCNQ2* epilepsy phenotypes. In 2020, in a novel model for *KCNQ2* encephalopathy generated by introducing the p. (Thr274Met) variant in C57Bl/6N mice, most of the pathophysiological features of the human disease have been successfully reproduced (Milh et al., 2020). Future studies on S-Lic efficacy on the *Kcnq2*^{p.(Thr274Met)/+} mouse model would therefore represent a helpful add-on.

4.6 | Potential role of eslicarbazepine acetate for the treatment of *KCNQ2*-related epilepsy

Currently, a disease-specific therapy against *KCNQ2*-related epilepsy does not exist, although in a clinical trial, the efficacy and tolerability of the K_v7 channel modulator **XEN496** (retigabine) are being tested (ClinicalTrials.gov, Identifier: NCT04639310; Millichap et al., 2016). Current treatments for *KCNQ2*-related epilepsies are based on administration of anti-epileptic drugs including sodium channel inhibitors, such as phenytoin or carbamazepine. While BFNE outcomes are mostly positive, patients suffering from *KCNQ2*-related severe encephalopathy often remain refractory to treatment (Kuersten et al., 2020). ESL has shown improved tolerability and safety compared to other dibenzazepine family members both in children and in adults (Almeida et al., 2008; Galiana et al., 2017; Rocamora, 2015). Moreover, multiple clinical trials have shown ESL to be effective in patients in whom other sodium channel blockers had failed (Ben-Menachem et al., 2010; Elger et al., 2009; Halász et al., 2010). The mechanisms for the improved efficacy of ESL include a lower affinity for the resting state of voltage-gated sodium channels and the ability to increase their slow, rather than fast, inactivation (Doeser et al., 2015; Hebeisen et al., 2015; Patrício Soares-da-Silva et al., 2015). These observations suggest a possibly enhanced efficacy of ESL to prevent seizures in paediatric and adult patients suffering from epilepsy refractory to standard treatment.

5 | CONCLUSIONS

Here, we investigated *in vitro* effects and *in vivo* efficacy of the novel anti-epileptic drug eslicarbazepine acetate in a *Kcnq2* mouse model of *KCNQ2*-related self-limited epilepsy. Our results indicate that hyperexcitability caused by a potassium channel mutation can be effectively targeted by an anti-seizure drug acting mainly on sodium channels. Our work confirms the anti-seizure efficacy of eslicarbazepine acetate in an *in vivo* mouse model of childhood epilepsy and furthermore points to important differences between *in vitro* and *in vivo* investigations in seizure and epilepsy models.

ACKNOWLEDGEMENTS

This work was supported by Eisai and BIAL Portela & Ca. LM and PF were partially funded by NeuroCure Cluster of Excellence, Berlin

Institute of Health. We would like to thank Mandy Marbler-Pötter for excellent technical assistance and Imandra Kempe for her contribution to the *in vitro* seizure-like events experiments.

AUTHOR CONTRIBUTIONS

PF, MH, MDW, and PSdS conceived the presented project idea. LM designed and performed *in vitro* and *in vivo* experiments and analysed the data. LK assisted with *in vivo* experiments and analyses. NM, MDW, and PF assisted with MATLAB analysis of *in vitro* experiments and interpretation. PSdS carried out ESL metabolite extraction. LM and PF wrote the manuscript and designed the figures. DS contributed to critical manuscript revision and supervision of data analysis. All authors discussed the results and commented on the manuscript.

CONFLICT OF INTEREST

Martin Holtkamp received speaker's honoraria and/or consultancy fees from Arvelle, Bial, Desitin, Eisai, GW Pharmaceuticals, UCB, and Zogenix within the last 3 years. The other authors declare no conflict of interest.

DECLARATION OF TRANSPARENCY AND SCIENTIFIC RIGOUR

This Declaration acknowledges that this paper adheres to the principles for transparent reporting and scientific rigour of preclinical research as stated in the *British Journal of Pharmacology* guidelines for [Design and Analysis](#) and [Animal Experimentation](#), and as recommended by funding agencies, publishers and other organisations engaged with supporting research.

DATA AVAILABILITY STATEMENT

The data that supports the findings of this study are also available from the corresponding author upon reasonable request.

ORCID

Laura Monni  <https://orcid.org/0000-0002-9513-6378>

Matthias Dipper-Wawra  <https://orcid.org/0000-0002-7311-1823>

Patricio Soares-da-Silva  <https://orcid.org/0000-0002-2446-5078>

Nikolaus Maier  <https://orcid.org/0000-0001-5203-0736>

Dietmar Schmitz  <https://orcid.org/0000-0003-2741-5241>

Martin Holtkamp  <https://orcid.org/0000-0003-2258-1670>

Pawel Fidzinski  <https://orcid.org/0000-0001-6373-4763>

REFERENCES

- Alexander, S. P., Mathie, A., Peters, J. A., Veale, E. L., Striessnig, J., Kelly, E., Armstrong, J. F., Faccenda, E., Harding, S. D., Pawson, A. J., Southan, C., Davies, J. A., Aldrich, R. W., Attali, B., Baggetta, A. M., Becirovic, E., Biel, M., Bill, R. M., Catterall, W. A., ... Zhu, M. (2021). The Concise Guide to PHARMACOLOGY 2021/22: Ion channels. *British Journal of Pharmacology*, 178(S1), S157–S245. <https://doi.org/10.1111/bph.15539>
- Almeida, L., Minciu, I., Nunes, T., Butoianu, N., Falcão, A., Magureanu, S.-A., & Soares-Da-Silva, P. (2008). Pharmacokinetics, efficacy, and tolerability of eslicarbazepine acetate in children and adolescents with epilepsy. *Journal of Clinical Pharmacology*, 48(8), 966–977. <https://doi.org/10.1177/0091270008319706>

- Alves, G., Figueiredo, I., Castel-Branco, M., Lourenço, N., Falcão, A., Caramona, M., & Soares-da-Silva, P. (2008). Disposition of eslicarbazepine acetate in the mouse after oral administration. *Fundamental & Clinical Pharmacology*, 22(5), 529–536. <https://doi.org/10.1111/j.1472-8206.2008.00617.x>
- Atallah, B. V., & Scanziani, M. (2009). Instantaneous modulation of gamma oscillation frequency by balancing excitation with inhibition. *Neuron*, 62(4), 566–577. <https://doi.org/10.1016/j.neuron.2009.04.027>
- Avoli, M., Psarropoulou, C., Tancredi, V., & Fueta, Y. (1993). On the synchronous activity induced by 4-aminopyridine in the CA3 subfield of juvenile rat hippocampus. *Journal of Neurophysiology*, 70(3), 1018–1029. <https://doi.org/10.1152/jn.1993.70.3.1018>
- Barker-Haliski, M., Löscher, W., Xiao, B., Brandt, C., Ravizza, T., Smolders, I., Xiao, B., Brandt, C., Löscher, W., & Harte-Hargrove, L. C. (2018). A companion to the preclinical common data elements for pharmacologic studies in animal models of seizures and epilepsy. A report of the TASK3 Pharmacology Working Group of the ILAE/AES Joint Translational Task Force. *Epilepsia Open*, 3, 53–68. <https://doi.org/10.1002/epi4.12254>
- Barton, M. E., Klein, B. D., Wolf, H. H., & White, H. S. (2001). Pharmacological characterization of the 6 Hz psychomotor seizure model of partial epilepsy. *Epilepsy Research*, 47(3), 217–227. [https://doi.org/10.1016/S0920-1211\(01\)00302-3](https://doi.org/10.1016/S0920-1211(01)00302-3)
- Beckonert, N. M., Opitz, T., Pitsch, X., da Silva, P. S., & Beck, H. (2018). Polyamine modulation of anticonvulsant drug response: A potential mechanism contributing to pharmacoresistance in chronic epilepsy. *Journal of Neuroscience*, 38(24), 5596–5605. <https://doi.org/10.1523/JNEUROSCI.0640-18.2018>
- Benes, J., Parada, A., Figueiredo, A. A., Alves, P. C., Freitas, A. P., Learmonth, D. A., Cunha, R. A., Garrett, J., & Soares-Da-Silva, P. (1999). Anticonvulsant and Sodium Channel-blocking properties of novel 10,11-dihydro-5H-dibenz[b,f]azepine-5-carboxamide derivatives. *Journal of Medicinal Chemistry*, 42(14), 2582–2587. <https://doi.org/10.1021/jm980627g>
- Ben-Menachem, E., Gabbai, A. A., Hufnagel, A., Maia, J., Almeida, L., & Soares-da-Silva, P. (2010). Eslicarbazepine acetate as adjunctive therapy in adult patients with partial epilepsy. *Epilepsy Research*, 89(2–3), 278–285. <https://doi.org/10.1016/j.eplepsyres.2010.01.014>
- Bokil, H., Andrews, P., Kulkarni, J. E., Mehta, S., & Mitra, P. P. (2010). Chronux: A platform for analyzing neural signals. *Journal of Neuroscience Methods*, 192(1), 146–151. <https://doi.org/10.1016/j.jneumeth.2010.06.020>
- Booker, S. A., Pires, N., Cobb, S., Soares-Da-Silva, P., & Vida, I. (2015). Carbamazepine and oxcarbazepine, but not eslicarbazepine, enhance excitatory synaptic transmission onto hippocampal CA1 pyramidal cells through an antagonist action at adenosine A1 receptors. *Neuropharmacology*, 93, 103–115. <https://doi.org/10.1016/j.neuropharm.2015.01.019>
- Bragin, A., Jando, G., Nadasdy, Z., Hetke, J., Wise, K., & Buzsáki, G. (1995). Gamma (40–100 Hz) oscillation in the hippocampus of the behaving rat. *Journal of Neuroscience*, 15(11), 47–60. <https://doi.org/10.1523/jneurosci.15-01-00047.1995>
- Brown, D. A., & Adams, P. R. (1980). Muscarinic suppression of a novel voltage-sensitive K⁺ current in a vertebrate neurone. *Nature*, 283(5748), 673–676. <http://www.ncbi.nlm.nih.gov/pubmed/6965523>. <https://doi.org/10.1038/283673a0>
- Brown, D. A., & Passmore, G. M. (2009). REVIEW neural KCNQ (Kv7) channels. *British Journal of Pharmacology*, 156, 1185–1195. <https://doi.org/10.1111/j.1476-5381.2009.00111.x>
- Brown, W. C., Schiffman, D. O., Swinyard, E. A., & Goodman, L. S. (1953). Comparative assay of an antiepileptic drugs by psychomotor seizure test and minimal electroshock threshold test. *The Journal of Pharmacology and Experimental Therapeutics*, 107(3), 273–283. <http://www.ncbi.nlm.nih.gov/pubmed/13035666>
- Buhl, E. H., Tamás, G., & Fisahn, A. (1998). Cholinergic activation and tonic excitation induce persistent gamma oscillations in mouse somatosensory cortex in vitro. *Journal of Physiology*, 513(1), 117–126. <https://doi.org/10.1111/j.1469-7793.1998.117by.x>
- Buzsáki, G. (1986). Hippocampal sharp waves: Their origin and significance. *Brain Research*, 398(2), 242–252. [https://doi.org/10.1016/0006-8993\(86\)91483-6](https://doi.org/10.1016/0006-8993(86)91483-6)
- Buzsáki, G. (2015). Hippocampal sharp wave-ripple: A cognitive biomarker for episodic memory and planning. *Hippocampus*, 25(10), 1073–1188. <https://doi.org/10.1002/hipo.22488>
- Buzsáki, G., & Wang, X.-J. (2012). Mechanisms of gamma oscillations. *Annual Review of Neuroscience*, 35(1), 203–225. <https://doi.org/10.1146/annurev-neuro-062111-150444>
- Colgin, L. L., Denninger, T., Fyhn, M., Hafting, T., Bonnevie, T., Jensen, O., Moser, M.-B., & Moser, E. I. (2009). Frequency of gamma oscillations routes flow of information in the hippocampus. *Nature*, 462(7271), 353–357. <https://doi.org/10.1038/nature08573>
- Cooper, E. C., Harrington, E., Jan, Y. N., & Jan, L. Y. (2001). M channel KCNQ2 subunits are localized to key sites for control of neuronal network oscillations and synchronization in mouse brain. *Journal of Neuroscience*, 21(24), 9529–9540. <https://doi.org/10.1523/jneurosci.21-24-09529.2001>
- Csicsvari, J., Jamieson, B., Wise, K. D., & Buzsáki, G. (2003). Mechanisms of gamma oscillations in the hippocampus of the behaving rat. *Neuron*, 37(2), 311–322. [https://doi.org/10.1016/S0896-6273\(02\)01169-8](https://doi.org/10.1016/S0896-6273(02)01169-8)
- Curtis, M. J., Alexander, S., Cirino, G., Docherty, J. R., George, C. H., Giembycz, M. A., Hoyer, D., Insel, P. A., Izzo, A. A., Ji, Y., MacEwan, D. J., Sobey, C. G., Stanford, S. C., Teixeira, M. M., Wonnacott, S., & Ahluwalia, A. (2018). Experimental design and analysis and their reporting II: Updated and simplified guidance for authors and peer reviewers. *British Journal of Pharmacology*, 175, 987–993. John Wiley and Sons Inc. <https://doi.org/10.1111/bph.14153>
- Delmas, P., & Brown, D. A. (2005). Pathways modulating neural KCNQ/M (Kv7) potassium channels. *Nature Reviews*, 6, 850–862. <https://doi.org/10.1038/nrn1785>
- Devaux, J. J., Kleopa, K. A., Cooper, E. C., & Scherer, S. S. (2004). KCNQ2 is a nodal K⁺ channel. *Journal of Neuroscience*, 24(5), 1236–1244. <https://doi.org/10.1523/JNEUROSCI.4512-03.2004>
- Doerer, A., Dickhof, G., Reitze, M., Uebachs, M., Schaub, C., Pires, N. M., Bonifácio, M. J., Soares-da-Silva, P., & Beck, H. (2015). Targeting pharmacoresistant epilepsy and epileptogenesis with a dual-purpose antiepileptic drug. *Brain*, 138(2), 371–387. <https://doi.org/10.1093/brain/awu339>
- Dunham, N. W., & Miya, T. S. (1957). A note on a simple apparatus for detecting neurological deficit in rats and mice**College of Pharmacy, University of Nebraska, Lincoln 8. *Journal of the American Pharmaceutical Association (Scientific Ed.)*, 46(3), 208–209. <https://doi.org/10.1002/jps.3030460322>
- EC50 Calculator|AAT Bioquest. Retrieved November 24, 2020, from <https://www.aatbio.com/tools/ec50-calculator>
- Elger, C., Halász, P., Maia, J., Almeida, L., & Soares-Da-Silva, P. (2009). Efficacy and safety of eslicarbazepine acetate as adjunctive treatment in adults with refractory partial-onset seizures: A randomized, double-blind, placebo-controlled, parallel-group phase III study. *Epilepsia*, 50(3), 454–463. <https://doi.org/10.1111/j.1528-1167.2008.01946.x>
- EpilepsyDiagnosis.org. Retrieved April 28, 2021, from <https://www.epilepsydiagnosis.org/>
- Fidzinski, P., Korotkova, T., Heidenreich, M., Maier, N., Schuetze, S., Kobler, O., Zuschratter, W., Schmitz, D., Ponomarenko, A., & Jentsch, T. J. (2015). KCNQ5 K⁺ channels control hippocampal synaptic inhibition and fast network oscillations. *Nature Communications*, 6, 6254. <https://doi.org/10.1038/ncomms7254>
- Fiest, K. M., Sauro, K. M., Wiebe, S., Patten, S. B., Kwon, C. S., Dykeman, J., Pringsheim, T., Lorenzetti, D. L., & Jetté, N. (2017). Prevalence and incidence of epilepsy. *Neurology Lippincott Williams*

- and Wilkins, 88, 296–303. <https://doi.org/10.1212/WNL.0000000000003509>
- Finney, D. J. (1971). Probit analysis. *Journal of Pharmaceutical Sciences*, 60(9), 1432. <https://doi.org/10.1002/jps.2600600940>
- Fisahn, A., Pike, F. G., Buhl, E. H., & Paulsen, O. (1998). Cholinergic induction of network oscillations at 40 Hz in the hippocampus in vitro. *Nature*, 394(6689), 186–189. <https://doi.org/10.1038/28179>
- Freeman, W. J. (2007). Definitions of state variables and state space for brain-computer interface: Part 1. Multiple hierarchical levels of brain function. *Cognitive Neurodynamics*, 1(1), 3–14. <https://doi.org/10.1007/s11571-006-9001-x>
- Galiana, G. L., Gauthier, A. C., & Mattson, R. H. (2017). Eslicarbazepine acetate: A new improvement on a classic drug family for the treatment of partial-onset seizures. *Drugs in R&D* Springer International Publishing, 17, 329–339. <https://doi.org/10.1007/s40268-017-0197-5>
- Goto, A., Ishii, A., Shibata, M., Ihara, Y., Cooper, E. C., & Hirose, S. (2019). Characteristics of KCNQ2 variants causing either benign neonatal epilepsy or developmental and epileptic encephalopathy. *Epilepsia*, 60(9), 1870–1880. <https://doi.org/10.1111/epi.16314>
- Grinton, B. E., Heron, S. E., Pelekanos, J. T., Zuberi, S. M., Kivity, S., Afawi, Z., Williams, T. C., Casalaz, D. M., Yendle, S., Linder, I., Lev, D., Lerman-Sagie, T., Malone, S., Bassan, H., Goldberg-Stern, H., Stanley, T., Hayman, M., Calvert, S., Korczyn, A. D., ... Berkovic, S. F. (2015). Familial neonatal seizures in 36 families: Clinical and genetic features correlate with outcome. *Epilepsia*, 56(7), 1071–1080. <https://doi.org/10.1111/epi.13020>
- Haas, H. L., Schaerer, B., & Vosmansky, M. (1979). A simple perfusion chamber for the study of nervous tissue slices in vitro. *Journal of Neuroscience Methods*, 1(4), 323–325. [https://doi.org/10.1016/0165-0270\(79\)90021-9](https://doi.org/10.1016/0165-0270(79)90021-9)
- Halász, P., Cramer, J. A., Hodoba, D., Czàonkowska, A., Guekht, A., Maia, J., Elger, C., Almeida, L., Soares-da-Silva, P., & BIA-2093-301 Study Group. (2010). Long-term efficacy and safety of eslicarbazepine acetate: Results of a 1-year open-label extension study in partial-onset seizures in adults with epilepsy. *Epilepsia*, 51(10), 1963–1969. <https://doi.org/10.1111/j.1528-1167.2010.02660.x>
- Hebeisen, S., Pires, N., Loureiro, A. I., Bonifácio, M. J., Palma, N., Whyment, A., Spanswick, D., & Soares-Da-Silva, P. (2015). Eslicarbazepine and the enhancement of slow inactivation of voltage-gated sodium channels: A comparison with carbamazepine, oxcarbazepine and lacosamide. *Neuropharmacology*, 89, 122–135. <https://doi.org/10.1016/j.neuropharm.2014.09.008>
- Heuzeroth, H., Wawra, M., Fidzinski, P., Dag, R., & Holtkamp, M. (2019). The 4-aminopyridine model of acute seizures in vitro elucidates efficacy of new antiepileptic drugs. *Frontiers in Neuroscience*, 13(JUN), 1–12. <https://doi.org/10.3389/fnins.2019.00677>
- Hill, M. R. H., & Greenfield, S. A. (2011). The membrane chamber: A new type of in vitro recording chamber. *Journal of Neuroscience Methods*, 195(1), 15–23. <https://doi.org/10.1016/j.jneumeth.2010.10.024>
- Hirtz, D., Thurman, D. J., Gwinn-Hardy, K., Mohamed, M., Chaudhuri, A. R., & Zalutsky, R. (2007). How common are the “common” neurologic disorders? *Neurology*, 68(5), 326–337. <https://doi.org/10.1212/01.wnl.0000252807.38124.a3>
- Holtkamp, D., Opitz, T., Hebeisen, S., Soares-da-Silva, P., & Beck, H. (2018). Effects of eslicarbazepine on slow inactivation processes of sodium channels in dentate gyrus granule cells. *Epilepsia*, 59(8), 1492–1506. <https://doi.org/10.1111/epi.14504>
- Ihara, Y., Tomonoh, Y., Deshimaru, M., Zhang, B., Uchida, T., Ishii, A., & Hirose, S. (2016). Retigabine, a Kv7.2/Kv7.3-channel opener, attenuates drug-induced seizures in knock-in mice harboring Kcnq2 mutations. *PLoS ONE*, 11(2), e0150095. <https://doi.org/10.1371/journal.pone.0150095>
- Jentsch, T. J. (2000). Neuronal KCNQ potassium channels: Physiology and role in disease. *Nature Reviews. Neuroscience*, 1(October), 21–30. <https://doi.org/10.1038/35036198>
- Jiang, X., & Kopp-Schneider, A. (2015). Statistical strategies for averaging EC50 from multiple dose–response experiments. *Archives of Toxicology*, 89(11), 2119–2127. <https://doi.org/10.1007/s00204-014-1350-3>
- Józwiak, S., Veggiotti, P., Moreira, J., Gama, H., Rocha, F., & Soares-da-Silva, P. (2018). Effects of adjunctive eslicarbazepine acetate on neurocognitive functioning in children with refractory focal-onset seizures. *Epilepsy and Behavior*, 81, 1–11. <https://doi.org/10.1016/j.yebeh.2018.01.029>
- Kato, M., Yamagata, T., Kubota, M., Arai, H., Yamashita, S., Nakagawa, T., Fujii, T., Sugai, K., Imai, K., Uster, T., Chitayat, D., Weiss, S., Kashii, H., Kusano, R., Matsumoto, A., Nakamura, K., Oyazato, Y., Maeno, M., Nishiyama, K., ... Saitou, H. (2013). Clinical spectrum of early onset epileptic encephalopathies caused by KCNQ2 mutation. *Epilepsia*, 54(7), 1282–1287. <https://doi.org/10.1111/epi.12200>
- Kraus, L., Monni, L., Schneider, U. C., Onken, J., Spindler, P., Holtkamp, M., & Fidzinski, P. (2020). Preparation of acute human hippocampal slices for electrophysiological recordings. *Journal of Visualized Experiments*, 159, 61085. <https://doi.org/10.3791/61085>
- Kubota, D., Colgin, L. L., Casale, M., Brucher, F. A., & Lynch, G. (2003). Endogenous waves in hippocampal slices. *Journal of Neurophysiology*, 89(1), 81–89. <https://doi.org/10.1152/jn.00542.2002>
- Kuersten, M., Tacke, M., Gerstl, L., Hoelz, H., Stülpnagel, C. V., & Borggraefe, I. (2020). Antiepileptic therapy approaches in KCNQ2 related epilepsy: A systematic review. *European Journal of Medical Genetics* Elsevier Masson SAS, 10.1016/j.ejmg.2019.02.001 63, 103628.
- Leclercq, K., & Kaminski, R. M. (2015). Genetic background of mice strongly influences treatment resistance in the 6 Hz seizure model. *Epilepsia*, 56(2), 310–318. <https://doi.org/10.1111/epi.12893>
- Lilley, E., Stanford, S. C., Kendall, D. E., Alexander, S. P. H., Cirino, G., Docherty, J. R., George, C. H., Insel, P. A., Izzo, A. A., Ji, Y., Panettieri, R. A., Sobey, C. G., Stefanska, B., Stephens, G., Teixeira, M., & Ahluwalia, A. (2020). ARRIVE 2.0 and the British Journal of Pharmacology: Updated guidance for 2020. *British Journal of Pharmacology*, 177(16), 3611–3616. <https://doi.org/10.1111/BPH.15178>
- Lopantsev, V., & Avoli, M. (1998). Laminar organization of epileptiform discharges in the rat entorhinal cortex in vitro. *Journal of Physiology*, 509(3), 785–796. <https://doi.org/10.1111/j.1469-7793.1998.785bm.x>
- López-Rivera, J. A., Pérez-Palma, E., Symonds, J., Lindy, A. S., McKnight, D. A., Leu, C., Zuberi, S., Brunklaus, A., Möller, R. S., & Lal, D. (2020). A catalogue of new incidence estimates of monogenic neurodevelopmental disorders caused by de novo variants. *Brain*, 143, 1099–1105. <https://doi.org/10.1093/brain/awaa051>
- Losi, G., Marcon, I., Mariotti, L., Sessolo, M., Chiavegato, A., & Carmignoto, G. (2016). A brain slice experimental model to study the generation and the propagation of focally-induced epileptiform activity. *Journal of Neuroscience Methods*, 260, 125–131. <https://doi.org/10.1016/j.jneumeth.2015.04.001>
- Loureiro, A. I., Fernandes-Lopes, C., Wright, L. C., & Soares-da-Silva, P. (2011). Development and validation of an enantioselective liquid-chromatography/tandem mass spectrometry method for the separation and quantification of eslicarbazepine acetate, eslicarbazepine, R-licarbazepine and oxcarbazepine in human plasma. *Journal of Chromatography B: Analytical Technologies in the Biomedical and Life Sciences*, 879(25), 2611–2618. <https://doi.org/10.1016/j.jchromb.2011.07.019>
- Maier, N., & Kempter, R. (2017). Hippocampal sharp wave/ripple complexes—Physiology and mechanisms. *Cognitive neuroscience of memory consolidation*. Studies in neuroscience, psychology and behavioral

- economics (pp. 227–249). Springer. https://doi.org/10.1007/978-3-319-45066-7_14
- Maier, N., Morris, G., Jochenning, F. W., & Schmitz, D. (2009). An approach for reliably investigating hippocampal sharpwave-ripples in vitro. *PLoS ONE*, *4*(9), e6925. <https://doi.org/10.1371/journal.pone.0006925>
- Maier, N., Nimrich, V., & Draguhn, A. (2003). Cellular and network mechanisms underlying spontaneous sharp wave-ripple complexes in mouse hippocampal slices. *The Journal of Physiology*, *550*(Pt 3), 873–887. <https://doi.org/10.1113/jphysiol.2003.044602>
- Miceli, F., Soldovieri, M. V., Ambrosino, P., Barrese, V., Migliore, M., Cilio, M. R., & Tagliatalata, M. (2013). Genotype-phenotype correlations in neonatal epilepsies caused by mutations in the voltage sensor of K_v 7.2 potassium channel subunits. *Proceedings of the National Academy of Sciences*, *110*, 4386–4391. <https://doi.org/10.1073/pnas.1216867110>
- Milh, M., Roubertoux, P., Biba, N., Chavany, J., Spiga Ghata, A., Fulachier, C., Collins, S. C., Wagner, C., Roux, J. C., Yalcin, B., Félix, M. S., Molinari, F., Lenck-Santini, P. P., & Villard, L. (2020). A knock-in mouse model for KCNQ2-related epileptic encephalopathy displays spontaneous generalized seizures and cognitive impairment. *Epilepsia*, *61*, (5), 868–878. <https://doi.org/10.1111/epi.16494>
- Millichap, J. J., Park, K. L., Tsuchida, T., Ben-Zeev, B., Carmant, L., Flamini, R., Joshi, N., Levisohn, P. M., Marsh, E., Nangia, S., Narayanan, V., Ortiz-Gonzalez, X. R., Patterson, M. C., Pearl, P. L., Porter, B., Ramsey, K., McGinnis, E. L., Tagliatalata, M., Tracy, M., ... Cooper, E. C. (2016). KCNQ2 encephalopathy: Features, mutational hot spots, and ezogabine treatment of 11 patients. *Neurology: Genetics*, *2*(5), e96. <https://doi.org/10.1212/NXG.0000000000000096>
- Mitra, P., & Bokil, H. (2008). *Observed Brain Dynamics*. Oxford University Press. <https://doi.org/10.1093/acprof:oso/9780195178081.001.0001>
- Mody, I., Lambert, J. D. C., & Heinemann, U. (1987). Low extracellular magnesium induces epileptiform activity and spreading depression in rat hippocampal slices. *Journal of Neurophysiology*, *57*(3), 869–888. <https://doi.org/10.1152/jn.1987.57.3.869>
- Montgomery, S. M., & Buzsáki, G. (2007). Gamma oscillations dynamically couple hippocampal CA3 and CA1 regions during memory task performance. *Proceedings of the National Academy of Sciences of the United States of America*, *104*(36), 14495–14500. <https://doi.org/10.1073/pnas.0701826104>
- Nappi, P., Miceli, F., Soldovieri, M. V., Ambrosino, P., Barrese, V., & Tagliatalata, M. (2020). Epileptic channelopathies caused by neuronal Kv7 (KCNQ) channel dysfunction. *Pflügers Archiv / European Journal of Physiology* Springer, *472*, 881–898. <https://doi.org/10.1007/s00424-020-02404-2>
- Ngugi, A. K., Bottomley, C., Kleinschmidt, I., Sander, J. W., & Newton, C. R. (2010). Estimation of the burden of active and life-time epilepsy: A meta-analytic approach. *Epilepsia*, *51*(5), 883–890. <https://doi.org/10.1111/j.1528-1167.2009.02481.x>
- Otto, J. F., Singh, N. A., Dahle, E. J., Leppert, M. F., Pappas, C. M., Pruess, T. H., Wilcox, K. S., & White, H. S. (2009). Electroconvulsive seizure thresholds and kindling acquisition rates are altered in mouse models of human KCNQ2 and KCNQ3 mutations for benign familial neonatal convulsions. *Epilepsia*, *50*(7), 1752–1759. <https://doi.org/10.1111/j.1528-1167.2009.02100.x>
- Papatheodoropoulos, C., & Kostopoulos, G. (2002). Spontaneous, low frequency (~2-3 Hz) field activity generated in rat ventral hippocampal slices perfused with normal medium. *Brain Research Bulletin*, *57*(2), 187–193. [https://doi.org/10.1016/S0361-9230\(01\)00738-9](https://doi.org/10.1016/S0361-9230(01)00738-9)
- Percie du Sert, N., Hurst, V., Ahluwalia, A., Alam, S., Avey, M. T., Baker, M., Browne, W. J., Clark, A., Cuthill, I. C., Dirnagl, U., Emerson, M., Garner, P., Holgate, S. T., Howells, D. W., Karp, N. A., Lázic, S. E., Lidster, K., MacCallum, C. J., Macleod, M., ... Würbel, H. (2020). The ARRIVE guidelines 2.0: Updated guidelines for reporting animal research. *Experimental Physiology*, *105*(9), 1459–1466. <https://doi.org/10.1113/EP088870>
- Perreault, P., & Avoli, M. (1992). 4-Aminopyridine-induced epileptiform activity and a GABA-mediated long-lasting depolarization in the rat hippocampus. *Journal of Neuroscience*, *12*(1), 104–115. <https://doi.org/10.1523/jneurosci.12-01-00104.1992>
- Pisano, T., Numis, A. L., Heavin, S. B., Weckhuysen, S., Angriman, M., Suls, A., Podesta, B., Thibert, R. L., Shapiro, K. A., Guerrini, R., Scheffer, I. E., Marini, C., & Cilio, M. R. (2015). Early and effective treatment of KCNQ2 encephalopathy. *Epilepsia*, *56*(5), 685–691. <https://doi.org/10.1111/epi.12984>
- Potschka, H., Soerensen, J., Pekcec, A., Loureiro, A., & Soares-da-Silva, P. (2014). Effect of eslicarbazepine acetate in the corneal kindling progression and the amygdala kindling model of temporal lobe epilepsy. *Epilepsy Research*, *108*(2), 212–222. <https://doi.org/10.1016/j.eplepsyres.2013.11.017>
- Racine, R. J. (1972). Modification of seizure activity by electrical stimulation: II. Motor seizure. *Electroencephalography and Clinical Neurophysiology*, *32*(3), 281–294. [https://doi.org/10.1016/0013-4694\(72\)90177-0](https://doi.org/10.1016/0013-4694(72)90177-0)
- Robbins, J., Passmore, G. M., Abogadie, F. C., Reilly, J. M., & Brown, D. A. (2013). Effects of KCNQ2 gene truncation on M-type Kv7 potassium currents. *PLoS ONE*, *8*(8), 1–6. <https://doi.org/10.1371/journal.pone.0071809>
- Rocamora, R. (2015). A review of the efficacy and safety of eslicarbazepine acetate in the management of partial-onset seizures. *Therapeutic Advances in Neurological Disorders* SAGE Publications, *8*, 178–186. <https://doi.org/10.1177/1756285615589711>
- Rudy, B. (1988). Diversity and ubiquity of K channels. *Neuroscience*, *25*(3), 729–749. [https://doi.org/10.1016/0306-4522\(88\)90033-4](https://doi.org/10.1016/0306-4522(88)90033-4)
- Sands, T. T., Balestri, M., Bellini, G., Mulkey, S. B., Danhaive, O., Bakken, E. H., Tagliatalata, M., Oldham, M. S., Vigeveno, F., Holmes, G. L., & Cilio, M. R. (2016). Rapid and safe response to low-dose carbamazepine in neonatal epilepsy. *Epilepsia*, *57*(12), 2019–2030. <https://doi.org/10.1111/epi.13596>
- Scharfman, H. E., & MacLusky, N. J. (2006). The influence of gonadal hormones on neuronal excitability, seizures, and epilepsy in the female. *Epilepsia NIH Public Access*, *47*, 1423–1440. <https://doi.org/10.1111/j.1528-1167.2006.00672.x>
- Schneider, J., Lewen, A., Ta, T. T., Galow, L. V., Isola, R., Papageorgiou, I. E., & Kann, O. (2015). A reliable model for gamma oscillations in hippocampal tissue. *Journal of Neuroscience Research*, *93*(7), 1067–1078. <https://doi.org/10.1002/jnr.23590>
- Sierra-Paredes, G., Loureiro, A. I., Wright, L. C., Sierra-Marcuño, G., & Soares-da-Silva, P. (2014). Effects of eslicarbazepine acetate on acute and chronic latrunculin A-induced seizures and extracellular amino acid levels in the mouse hippocampus. *BMC Neuroscience*, *15*(1), 134. <https://doi.org/10.1186/s12868-014-0134-2>
- Singh, N. A., Otto, J. F., Jill Dahle, E., Pappas, C., Leslie, J. D., Leslie, J. D., Vilaythong, A., Noebels, J. L., White, H. S., Wilcox, K. S., & Leppert, M. F. (2008). Mouse models of human KCNQ2 and KCNQ3 mutations for benign familial neonatal convulsions show seizures and neuronal plasticity without synaptic reorganization. *Journal of Physiology*, *586*(14), 3405–3423. <https://doi.org/10.1113/jphysiol.2008.154971>
- Soares-da-Silva, P., Pires, N., Bonifácio, M. J., Loureiro, A. I., Palma, N., & Wright, L. C. (2015). Eslicarbazepine acetate for the treatment of focal epilepsy: An update on its proposed mechanisms of action. *Pharmacology Research & Perspectives*, *3*(2), e00124. <https://doi.org/10.1002/prp2.124>
- Symonds, J. D., Zuberi, S. M., Stewart, K., McLellan, A., O'Regan, M., MacLeod, S., Jollands, A., Joss, S., Kirkpatrick, M., Brunklaus, A., Pilz, D. T., Shetty, J., Dorris, L., Abu-Arafah, I., Andrew, J., Brink, P., Callaghan, M., Cruden, J., Diver, L. A., ... Wilson, M. (2019). Incidence and phenotypes of childhood-onset genetic epilepsies: A prospective population-based national cohort. *Brain: A Journal of Neurology*, *142*(8), 2303–2318. <https://doi.org/10.1093/brain/awz195>

- Traynelis, S. F., & Dingledine, R. (1988). Potassium-induced spontaneous electrographic seizures in the rat hippocampal slice. *Journal of Neurophysiology*, 59(1), 259–276. <https://doi.org/10.1152/jn.1988.59.1.259>
- Trinka, E., Ben-Menachem, E., Kowacs, P. A., Elger, C., Keller, B., Löffler, K., Rocha, J. F., & Soares-da-Silva, P. (2018). Efficacy and safety of eslicarbazepine acetate versus controlled-release carbamazepine monotherapy in newly diagnosed epilepsy: A phase III double-blind, randomized, parallel-group, multicenter study. *Epilepsia*, 59(2), 479–491. <https://doi.org/10.1111/epi.13993>
- Trompoukis, G., Rigas, P., Leontiadis, L. J., & Papatheodoropoulos, C. (2020). Ih, GIRK, and KCNQ/Kv7 channels differently modulate sharp wave-ripples in the dorsal and ventral hippocampus. *Molecular and Cellular Neuroscience*, 107, 103531. <https://doi.org/10.1016/j.mcn.2020.103531>
- Vittinghoff, E., & McCulloch, C. E. (2007). Relaxing the rule of ten events per variable in logistic and cox regression. *American Journal of Epidemiology*, 165(6), 710–718. <https://doi.org/10.1093/aje/kwk052>
- Wang, H. S., Pan, Z., Shi, W., Brown, B. S., Wymore, R. S., Cohen, I. S., Dixon, J. E., & McKinnon, D. (1998). KCNQ2 and KCNQ3 potassium channel subunits: Molecular correlates of the M-channel. *Science*, 282(5395), 1890–1893. <https://doi.org/10.1126/science.282.5395.1890>
- Watanabe, H., Nagata, E., Kosakai, A., Nakamura, M., Yokoyama, M., Tanaka, K., & Sasai, H. (2000). Disruption of the epilepsy KCNQ2 gene results in neural hyperexcitability. *Journal of Neurochemistry*, 75(1), 28–33. <https://doi.org/10.1046/j.1471-4159.2000.0750028.x>
- Weckhuysen, S., Mandelstam, S., Suls, A., Audenaert, D., Deconinck, T., Claes, L. R. F., Deprez, L., Smets, K., Hristova, D., Jordanova, I., Jordanova, A., Ceulemans, B., Jansen, A., Hasaerts, D., Roelens, F., Lagae, L., Yendle, S., Stanley, T., Heron, S. E., ... De Jonghe, P. (2012). KCNQ2 encephalopathy: Emerging phenotype of a neonatal epileptic encephalopathy. *Annals of Neurology*, 71(1), 15–25. <https://doi.org/10.1002/ana.22644>
- Wheless, J. W., Fulton, S. P., & Mudigoudar, B. D. (2020). Dravet syndrome: A review of current management. *Pediatric Neurology Elsevier Inc*, 107, 28–40. <https://doi.org/10.1016/j.pediatrneurol.2020.01.005>
- Wójtowicz, A. M., van den Boom, L., Chakrabarty, A., Maggio, N., Haq, R. U., Behrens, C. J., & Heinemann, U. (2009). Monoamines block kainate- and carbachol-induced. γ -oscillations but augment stimulus-induced γ -oscillations in rat hippocampus in vitro. *Hippocampus*, 19(3), 273–288. <https://doi.org/10.1002/hipo.20508>
- XEN496 (Ezogabine) in children with KCNQ2 developmental and epileptic encephalopathy—Full text view—ClinicalTrials.gov. Retrieved May 17, 2021, from <https://clinicaltrials.gov/ct2/show/study/NCT04639310>
- Zarnadze, S., Bäuerle, P., Santos-Torres, J., Böhm, C., Schmitz, D., Geiger, J. R., Dugladze, T., & Gloveli, T. (2016). Cell-specific synaptic plasticity induced by network oscillations. *eLife*, 5(MAY2016), e14912. <https://doi.org/10.7554/eLife.14912>

SUPPORTING INFORMATION

Additional supporting information may be found in the online version of the article at the publisher's website.

How to cite this article: Monni, L., Kraus, L., Dipper-Wawra, M., Soares-da-Silva, P., Maier, N., Schmitz, D., Holtkamp, M., & Fidzinski, P. (2022). *In vitro* and *in vivo* anti-epileptic efficacy of eslicarbazepine acetate in a mouse model of KCNQ2-related self-limited epilepsy. *British Journal of Pharmacology*, 179(1), 84–102. <https://doi.org/10.1111/bph.15689>